INFORMATION TO USERS

This manuscript has been reproduced from the microfilm master. UMI films the text directly from the original or copy submitted. Thus, some thesis and dissertation copies are in typewriter face, while others may be from any type of computer printer.

The quality of this reproduction is dependent upon the quality of the copy submitted. Broken or indistinct print, colored or poor quality illustrations and photographs, print bleedthrough, substandard margins, and improper alignment can adversely affect reproduction.

In the unlikely event that the author did not send UMI a complete manuscript and there are missing pages, these will be noted. Also, if unauthorized copyright material had to be removed, a note will indicate the deletion.

Oversize materials (e.g., maps, drawings, charts) are reproduced by sectioning the original, beginning at the upper left-hand corner and continuing from left to right in equal sections with small overlaps.

ProQuest Information and Learning
300 North Zeeb Road, Ann Arbor, MI 48106-1346 USA
800-521-0600

N.M.R. BELOW 1 K WITH A S.Q.U.I.D. MAGNETOMETER

by

M.D. O'Connell

Submitted to the School of Graduate Studies
in partial fulfilment of the requirements
for the degree of Master of Science

Department of Physics
Faculty of Science and Engineering
The University of Ottawa
Ottawa, Canada

1977

ABSTRACT

A SQUID magnetometer has been used to study the N.M.R. signal and the relaxation time of normal aluminum in low magnetic fields as a function of temperature for the purpose of doing thermometry below 1K. The variation of signal amplitude with temperatures and r.f. power is found to agree with the predictions from the Bloch equations. A description is given of the cryostat that used a circulating helium gas heat exchanger to cool the experimental stage to 1.3K and adiabatic demagnetization of a paramagnetic salt to further cool the stage to 240 mK.

The N.M.R. spectrum of lithium in a crystal of lithium niobate was also studied at 4.2K. The quadrupole coupling constant e^2qQ/h was measured to be 52 $\pm$ 1 KHz and is compared to previous results.

The design of a new cryostat to operate below 100 mK to replace the current one in use is discussed. The construction and operation of a liquid helium level indicator is discussed and commented on.

ACKNOWLEDGMENT

The author wishes to thank Dr. G. Lamarche for his interest and assistance in this work; Drs. C. Benson, A. Manoogian, P. Rochon and J.C. Woolley; R.G. Goodchild, L.M. Emery, A. Roth and C. Francois for their help and enlightening conversations.

He would also like to thank the people in the Machine Shop for the expert work in making the cryostat, Mrs. M.E. O'Connell for the typing of the manuscript and all the patient people who have waited, especially my wife Margaret.

TABLE OF CONTENT

	Page
ABSTRACT	ii
ACKNOWLEDGMENT	iii
LIST OF FIGURES	vi
INTRODUCTION	1
CHAPTER I - Theory	
SQUID	8
Principle of the Method	8
Theory	
Aluminum	9
Lithium Niobate	16
CHAPTER II - Experimental Apparatus and Procedure	
Introduction	19
Apparatus	23
(1) Dewars	23
(2) 4.2K Environment	25
(3) 1.3K Refrigerator	26
(4) Experimental Stage	32
(5) Salt Pill	34
(6) Gas Heat Exchanger	35
(7) Carbon Resistance Thermometers	37
(8) N.M.R. Head	46
(9) Solenoid and Magnetic Shielding	51

	Page
Procedure	
Introduction	56
(a) Preparation of Cryostat	56
(b) Precooling to Liquid Nitrogen Temperature	57
(c) Liquid Helium Transfer	59
(d) Adiabatic Demagnetization Cooling	61
(e) N.M.R. Signal	62
CHAPTER III - Cooling Below 1K Results	64
CHAPTER IV - Aluminum Results	
Introduction	69
Experimental Results	72
Discussion	77
CHAPTER V - Lithium Niobate Results	
Introduction	82
Results	83
Discussion	86
CHAPTER VI - Conclusion	89
BIBLIOGRAPHY	98
APPENDIX	101
CALIBRATION TABLE OF C.R.T. UPPER	105
CALIBRATION TABLE OF C.R.T. LOWER	107

LIST OF FIGURES

		Page
Figure 1.	Block Diagram of Experiment	9
Figure 2.	Schematic Diagram of Cryostat	20
Figure 3.	Calorimeter	24
Figure 4.	Impedence Measuring Set-up	28
Figure 5.	Variation of Z With Pressure	29
Figure 6.	Heat Exchanger	36
Figure 7.	Resistor Platelet	40
Figure 8.	Carbon Resistor Thermometer Assembly	40
Figure 9.	Schematic of Resistance Bridge	41
Figure 10.	Wiring Diagram of Bridge	41
Figure 11.	Calibration Curve R_{upper}	42
Figure 12.	Calibration Curve R_{lower}	43
Figure 13.	N.M.R. Head	48
Figure 14.	Stycast Seal	49
Figure 15.	Field Profile (Vertical) of Helmholtz Pair	54
Figure 16.	Field Profile (Horizontal) of Helmholtz Pair	55
Figure 17.	Temperature versus Time Curve, Lower Stage	66
Figure 18.	Typical N.M.R. Tracing, Al Foil	73

		Page
Figure 19.	Typical N.M.R. Tracing, Al Powder	74
Figure 20.	Relaxation Time, Al Powder	76
Figure 21.	Graph of Saturation Versus r.f. Amplitude, Al Powder	78
Figure 22.	Field Profile, r.f. Coil	79
Figure 23.	Typical N.M.R. Tracing, $LiNbO_3$	84
Figure 24.	Proposed Calorimeter	93
Figure 25.	Details of Proposed Lower Stage	94
Figure 26.	Schematic of Liquid Helium Level Indicator	104

INTRODUCTION

This thesis can be divided into two main topics of study: (1) an investigation into the possibilities of using SQUID magnetometer detection of N.M.R. at very low temperatures for (a) thermometry and (b) weak signal enhancement, (2) the development of a specially designed adiabatic demagnetization cryostat to achieve the low temperature and a study of how to incorporate the SQUID and the SQUID elements in it.

The rapid development of methods of obtaining temperatures below 1K has accentuated the need for reliable thermometry. Originally these low temperatures were achieved only by adiabatic demagnetization of a paramagnetic salt. Now cooling can be accomplished by a ^{3}He-^{4}He dilution refrigerator, adiabatic compressional cooling of ^{3}He, and nuclear cooling. Each of the aforementioned methods have their advantages but whichever technique is used, the temperature or temperature change must be known accurately.

A convenient method of measuring temperature is the magnetic thermometer based on Curie's Law. SQUID magnetometers have been used to measure the

temperature dependent longitudinal changes in static magnetization of nuclear paramagnets and also of paramagnetic salts such as CMN. This type of thermometry, where the susceptibility is the temperature dependent variable, is a powerful measuring technique due to its simplicity. Normally this type of thermometer is calibrated in the higher temperature range (liquid helium) but this method does have its limitations because any change in the output of the SQUID i.e. flux jumps or base line drift, would invalidate the calibration.

Another approach is afforded by measurement of the N.M.R. signal height and spin-lattice relaxation time using a SQUID magnetometer. This method is in competition with conventional techniques. Two basic instruments have been used in this conventional method; the continuous wave which looks at signal amplitude, and the free precession decay method where both the amplitude and the relaxation time could be measured well down into the sub millikelvin range. This pulsed N.M.R. thermometer has been so developed by Walstedt, Hahn, Froidevaux and Geissler[1] and further improved by them and others to such a degree of precision that they are now available commercially.

An important aspect of N.M.R. thermometry

relates to the choice of nuclear species, its chemical state and the form it is to be used in. Metallic samples provide the best possibilities for thermal conduction and fast attainment of thermal equilibrium at very low temperatures and they have been investigated by many workers for this purpose. Quality of the sample is important because any magnetic impurities in some metals could cause a departure from Curie's Law. Metal samples can be used in one of several forms, either as a thin foil, as a powder or as a bundle of wires. Whichever form is used, the thickness exposed to r.f. radiation should be small compared to the skin depth. Factors that affect the choice are availability, ease of handling and the form that it is supplied in.

Aalto, Collan, Gylling and Nores[2] have constructed an N.M.R. thermometer where they used a series of r.f. pulses at the Larmor precession frequency to destroy the nuclear magnetization and observed the nuclear free precession signal on an oscilliscope as the nuclear temperature returned to equilibrium with the lattice temperature. This pulse method was employed to discriminate between the signal and the large coherent background of the magnetic impurities in the host metal, platinum. However, it is not clear whether or not this

rapid measurement technique actually extracts the N.M.R. signal from the background noise caused by the impurity in the sample. These impurities affect the line width of the resonance hence temperature behaviour of the magnetic impurities will adversely affect the performance of the nuclear spin signal as a thermometer as stated by Symko.[3]

A literature search showed that aluminum was the best choice to start a study.[4] In samples of similar volume, there will be more aluminum nuclei present than either of the copper isotopes, ^{63}Cu and ^{65}Cu, as the relative sensitivity of aluminum is greater than both isotopes of copper, it is expected to produce a larger signal. The ratio of amplitudes of the signals from ^{27}Al and from ^{63}Cu and ^{65}Cu is approximately 4:2:1. The relaxation time of ^{63}Cu and ^{27}Al are both relatively long, 1.23 s and 1.8 s respectively at 1K.[3] Also in a dilute aluminum alloy, magnetic impurities such as iron and manganese do not form local moments.[3]

A sample of lithium niobate was also studied in the present experimental apparatus. Lithium niobate is available in relatively perfect single crystal form and is currently used in many new sophisticated devices. Previous studies on the physical properties of the material have been done by conventional N.M.R.[5-11]

Our purpose then was to cool the crystal to very low temperatures to see if more and possibly new information could be gleaned from the study of the N.M.R. properties of $LiNbO_3$ with a SQUID magnetometer at these low temperatures.

A major portion of the work deals with the development of an adiabatic demagnetization cryostat that included a SQUID magnetometer and a small N.M.R. head located on the experimental stage. The technical problems that had to be solved arose because the normal operating temperature of the SQUID is 4.2K, whereas the N.M.R. head producing the signal is located on the experimental stage that operates below 1K.

Since the SQUID requires the bath temperature to be 4.2K, an effective continuously operating refrigerator and heat exchangers had to be developed that could cool the entire lower stage to at least 1.3K as the starting temperature if efficient cooling by adiabatic demagnetization of a paramagnetic salt is to be obtained.

One problem encountered was to design a vacuum tight seal for the leads from the superconducting flux transformer in the N.M.R. head to the SQUID. To interchange samples, the N.M.R. r.f. head had to be

removable thus necessitating a junction in the leads of the transformer and also in the leads to the r.f. coil. It was decided to incorporate both the seal and junction of the leads into a small box. The join must be superconducting but niobium wire leads cannot be soldered. The separation between the connections must be as small as possible to reduce the self-inductance of the leads and hence lessen the noise being introduced into the superconducting flux transformer.

Development of adequate shielding of the SQUID and the SQUID elements is extremely important as the amplitude of the desired signal is only a fraction of the changes in the earth's magnetic field.

In Chapter I of this thesis, we shall first briefly discuss the SQUID and the principle of the method used to obtain the N.M.R. signal, then we will consider its application to thermometry when the relevant signal is measured by slow passage, by fast passage and finally by an r.f. pulse technique to study the relaxation time. Chapter II will deal with the experimental apparatus, the procedure for cooling below 1K by adiabatic demagnetization and then the method of obtaining the N.M.R. tracings. Chapter III discusses the cooling results and an evaluation is done of the heat leak at the low

temperature. Chapter IV looks at the results for aluminum foil and aluminum powder at different temperatures and fields, B_o and finally compares the results to the theory. Chapter V covers the results of the lithium signal in lithium niobate with some comments on the purity of the crystal. The concluding remarks and design suggestions for a new cryostat is in Chapter VI. Included in this work as an Appendix is the description and the circuit diagram of a liquid helium level indicator together with some comments on its performance and precision.

CHAPTER I

SQUID

The theory and operation of an r.f. biased point contact SQUID has been excellently covered in the literature and in Lounasmaa's book and therefore will not be discussed here.[12]

With three copper shields and the stainless steel dewars protecting the experiment from any electrical noise, a single pick-up coil was used, instead of the gradiometer configuration used by Goodchild[13], in the N.M.R. magnetometer head to increase the amplitude of the signal.

PRINCIPLE OF THE METHOD

Nuclear magnetic resonance was observed by continuously monitoring the longitudinal magnetization of a sample placed in a constant magnetic field B_o, along the Z axis as the frequency of an r.f. field $B_1 \cos \omega t$, along the X axis is swept through the Larmor precession frequency ω_o (See Fig. #1). The sample was maintained at a constant temperature T, that could be varied between 240 mK to 4.2K for the purpose of investigating N.M.R. thermometry in this temperature range.

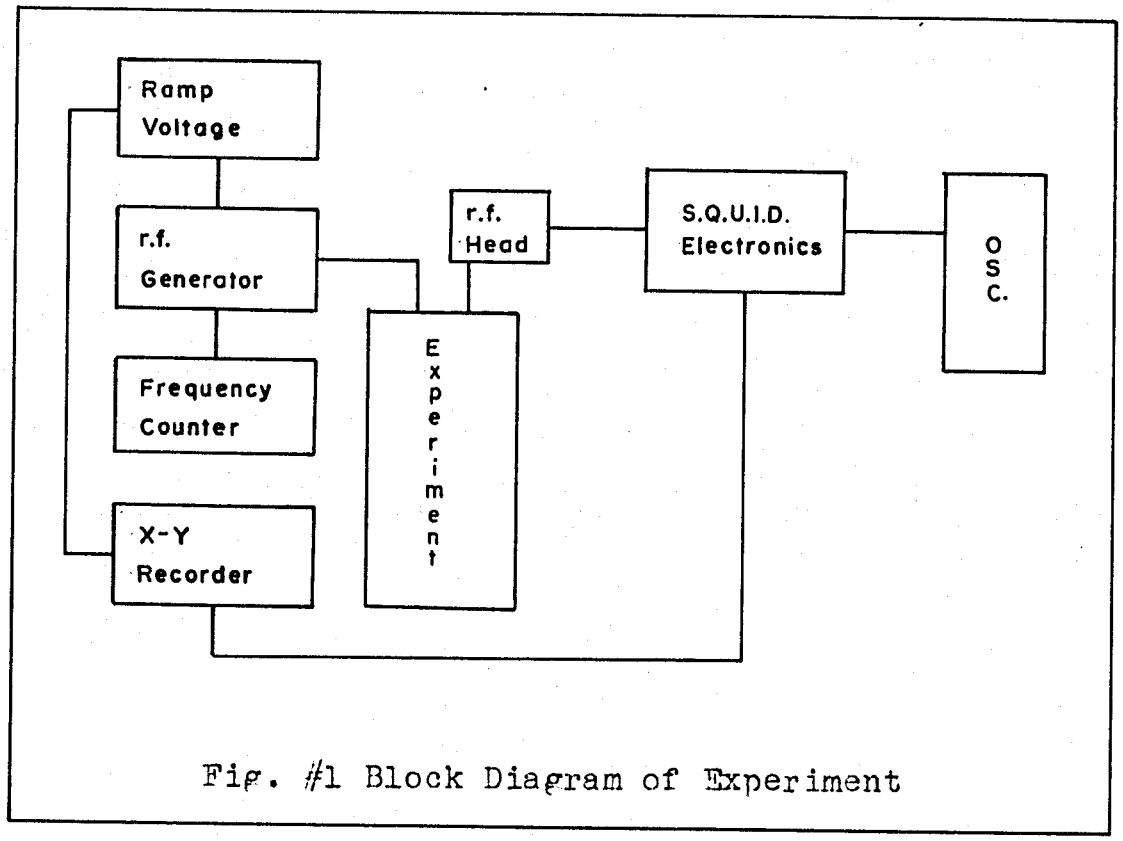

Fig. #1 Block Diagram of Experiment

THEORY

Aluminum

Many nuclei, in their ground state have non-zero angular momentum and a dipolar magnetic moment that gives rise to nuclear magnetism. Due to the smallness of the nuclear moments, magnetic coupling between the nuclear spins is such that temperatures in the order of 10^{-7}K or less will be needed for ordering to occur and the observation of ferromagnetism or antiferromagnetism (i.e. $\mu H \approx kT$). In the temperature range of interest here, the nuclei obey Curie's Law with great accuracy,

namely

$$M = \frac{N\gamma^2\hbar^2 I(I+1)B_o}{3kT_s} = \chi_o B_o \qquad (1)$$

or

$$M = \frac{CB_o}{T_s} \qquad (2)$$

where C is Curie's constant and T_s is the spin temperture. In so far as the spin system is in thermal equilibrium with its lattice, the temperature derived from the magnetization measurements is equal to T, the absolute temperature of the lattice down to at least 1 mK.

Now the Bloch equation of the motion of the nuclear magnetization of an ensemble of free spins in a homogeneous field H is

$$\frac{d\vec{M}}{dt} = \gamma\vec{M}x\vec{H} \qquad (3)$$

In a static field, $H_z = H_o$, the magnetization along Z, M_z relaxes to M_o in a characteristic time T_1 (the longitudinal relaxation time) and can be described by

$$\frac{dM_z}{dt} = -\frac{M_z - M_o}{T_1} \qquad (4)$$

Also if there is a perturbing r.f. field perpendicular to H_o, then there will be a component of the nuclear magnetization also at right angles to H_o. Since the

spins are not actually free, but interact with each other and their surroundings, the transverse magnetization will decay at a rate given by

$$\frac{dM_x}{dt} = -\frac{M_x}{T_2} \quad , \quad \frac{dM_y}{dt} = -\frac{M_y}{T_2} \qquad (5)$$

where T_2 is the transverse relaxation time.

The motion due to relaxation can be superimposed on the motion of the free spins giving

$$\frac{d\vec{M}}{dt} = \gamma\vec{M}\times\vec{H} - \frac{M_x\vec{i}' + M_y\vec{j}'}{T_2} - \frac{M_z - M_o}{T_1}\vec{k}' \qquad (6)$$

where $\vec{i}'$, $\vec{j}'$, & $\vec{k}'$ are the unit vectors in the lab frame of reference.

We shall now assume steady state conditions near saturation where the applied field is a sum of D.C. field.

$$H_z = H_o = -\frac{\omega_o}{\gamma} \qquad (7)$$

and an r.f. field $\bar{H}_1$ of amplitude $H_1 = -\omega_1/\gamma$ rotating at a frequency ω near ω_o. This field will be one of the rotating components of

$$H_x = 2H_1\cos(\omega t) \qquad (8)$$

In the frame rotating around H_z at the frequency ω, there will be an effective static field

$$\vec{H}_{eff} = \left(H_o + \frac{\omega}{\gamma}\right)\vec{k} + H_1\vec{i}$$

$$= \frac{(\omega - \omega_o)\vec{k} - \omega_1\vec{i}}{\gamma}$$

$$= \frac{\Delta\omega\vec{k} - \omega_1\vec{i}}{\gamma} \qquad (9)$$

where $\vec{i}$, $\vec{j}$, $\vec{k}$ are the unit vectors in the rotating frame of reference. In this rotating frame, the equation of motion (6) is now

$$\frac{d\vec{M}}{dt} = \gamma(\vec{M}\times\vec{H}_{eff}) - \frac{(M'_x\vec{i} + M'_y\vec{j})}{T_2} - \frac{(M_z - M_o)}{T_1}\cdot\vec{k} \qquad (10)$$

where $M'x$ and $M'y$ are the tranverse components of $\vec{M}$ in the rotating frame. Equation (10) can be rewritten as

$$\frac{dM'_x}{dt}\cdot\vec{i} + \frac{dM'_y}{dt}\cdot\vec{j} + \frac{dM_z}{dt}\cdot\vec{k} =$$

$$(M'_x\vec{i} + M'_y\vec{j} + M_z\vec{k})\times(\Delta\omega\vec{k} - \omega_1\vec{i})$$

$$- \frac{(M'_x\vec{i} + M'_y\vec{j})}{T_2} - \frac{(M_z - M_o)}{T_1}\cdot\vec{k} \qquad (11)$$

or

$$\frac{dM'_x}{dt} = -\frac{M'_x}{T_2} + \Delta\omega M'_y \qquad (12)$$

$$\frac{dM'_y}{dt} = -\Delta\omega M'_x - \frac{M'_y}{T_2} - \omega_1 M_z \qquad (13)$$

$$\frac{dM_z}{dt} = \omega_1 M'_y - \frac{(M_z - M_o)}{T_1} \qquad (14)$$

We can obtain steady state solutions by setting

$$\frac{dM'_x}{dt} = \frac{dM'_y}{dt} = \frac{dM_z}{dt} = 0 \qquad (15)$$

and solving the three ensuing equations. Since the pick-up coil in the N.M.R. magnetometer head is aligned in the Z direction, only changes in the M_z will be detected, that is

$$M_z = \frac{(1 + (\Delta\omega T_2)^2) M_o}{1 + (\Delta\omega T_2)^2 + \gamma^2 H_1^2 T_1 T_2} \qquad (16)$$

at resonance, $\Delta\omega = o$, i.e. $\omega = \omega_o$, and

$$M_z = \frac{M_o}{1 + \gamma^2 H_1^2 T_1 T_2} \qquad (17)$$

As the SQUID only detects changes in magnetization, we are interested only in $\Delta Mz = M_o - M_z$ which is proportional to S.H., the signal amplitude from the SQUID electronics.

$$S.H. \; \alpha \; \frac{M_o \gamma^2 H_1^2 T_1 T_2}{1 + \gamma^2 H_1^2 T_1 T_2} \qquad (18)$$

Equation (18) affords us an easy determination of the field factor for H_1 simply by plotting a graph of S.H. versus current to the r.f. coil and finding the corresponding current at half the saturation value, then

$$\gamma^2 H_1^2 T_1 T_2 = 1 \qquad (19)$$

In the case of a metal, T_1 can be replaced by the Korringa relation

$$T_1 T = K \qquad (20)$$

But it must be remembered that K is field dependent i.e.

$$T_1(B) = T_1 \left[\frac{B^2 + b^2}{B^2 + 2b^2}\right] \qquad (21)$$

Where T_1 is the high field value. The constant K can vary from 1.8 K-s at high field (B>10 mT) to 0.7 K-s at zero field.

Since the nuclei are expected to obey Curie's Law down below 1 mK, M_o in equation (18) can be replaced to yield

$$S.H. \alpha \frac{\gamma^2 H_1^2 K T_2 B_o}{T(T + \gamma^2 H_1^2 K T_2)} \qquad (22)$$

which is valid for slow passage through resonance. This is the equation of Meredith et al[14], which for a given B_o, the signal height is proportional to T^{-2} for low power and T^{-1} at high power.

It is important that eddy current heating in the sample is kept small in order not to disturb the temperature of the lattice. The eddy current heating, $\dot{Q}$, of a powder sample comprised of spheres, by an r.f.

of amplitude B_1, assuming full penetration is[1]

$$\dot{Q} = 7.5\sigma\omega^2 R^2 B_1^2 V \qquad (23)$$

As $\dot{Q}$ is proportional to the square of B_1, it is very important to keep B_1 as small as possible. The eddy current heating in the powdered aluminum of an average radius of 40 μm, where B_1 is 20 μT oscillating at 125 KHz is 0.31 μW. However, not only is the sample warmed by eddy current heating, but also the r.f. coil itself and the r.f. shield, which in turn would also raise the temperature of the sample and entire lower stage.

By only having the r.f. on for short times (i.e. approximately 1s) to do a measurement of T_1, the heating will be much less than using a continuous wave method.

The relaxation time T_1, can be measured by doing an adiabatic fast passage and then turning off the r.f. and record the corresponding relaxation or a short duration pulse of the order of 1 second may be used. In the first case, the change in magnetization will be 2 M_z since we are giving a 180° pulse to the spins with a temperature of -Ts and the second case, the maximum change will be M_z since we are not integrating all the contributions to the magnetization.

The relaxation will be of the form

$$M_z = M_o(1 - 2\exp(-t/T_1)) \qquad (24)$$

which is a solution to equation (4). T_1 can be obtained from a graph of $\ln M_z$ vs t.

Due to the extreme sensitivity of the SQUID, the temperature dependence of the electronic magnetization of the sample from skin depth effects may be detected by the SQUID. This would result in a dispersive type of behaviour, i.e. a drift-like shift in the base line and the peaks to be displaced by an amount less than 1KHz[15]. This effect would be most noticeable in the aluminum foil sample as the thickness was three times the skin depth.

Pauli[16] showed that the correct form of the magnetization due to the conduction electrons is

$$M \doteq \frac{N\mu^2 B}{kT} \cdot \frac{T}{T_F} = \frac{N\mu^2 B}{kT_F} \qquad (25)$$

which is independent of temperature. The calculated magnetization is $3 \times 10^{-4}\ \Phi_o$ which is less than the lowest detectable signal by the SQUID, $0.01\Phi_o$ and, hence the magnetization and any temperature variation will not be observed.

LITHIUM NIOBATE

For a nucleus of spin $\vec{I}$, a magnetic moment

$\vec{\mu} = \gamma h \vec{I}$, and an electric quadrupole moment eQ, located in an axially symmetric gradient of strength $eq = \partial E_z/\partial z$, where z is the principle axis of the field gradient tensor and in a magnetic field Bo aligned along z, there will be one central peak given by

$$\upsilon_{\pm\frac{1}{2} \rightarrow \mp\frac{1}{2}} = \gamma B_o \qquad (26)$$

Both lithium and niobium have a quadrupole moment, for ^{7}Li, I = 3/2 and there will be two equally spaced satellite peaks separated from the main peak by

$$\Delta\nu = \pm \frac{e^2qQ}{h} \frac{(3\cos^2\theta - 1)}{2} \qquad (27)$$

where θ is the angle between the major field gradient direction and B_o, and e^2qQ/h is the quadrupole coupling constant. For ^{93}Nb, I = 9/2 and there will be eight satellite peaks and one main peak.

The intensity of the line corresponding to $m \leftrightarrow m-1$ transition is proportional to the transition probability, that is

$$S.H. \alpha I(I + 1) - m(m - 1) \qquad (28)$$

or alternately

$$S.H. \alpha (I + m)(I - m + 1) \qquad (28a)$$

The ratio of the signal heights then for the peaks corresponding to the following transitions, - 3/2 → - 1/2: - 1/2 → + 1/2: + 1/2 → + 3/2 are 3:4:3.

This is not rigourously correct but it is a good approximation.

CHAPTER II

EXPERIMENTAL APPARATUS

INTRODUCTION

The cryostat used in this work to obtain temperatures below 1K by adiabatic demagnetization of a paramagnetic salt, is, on the whole, of conventional design (cf. Lounasmaa (1975) and references cited therein). It incorporates a 1K plate inside the vacuum chamber to which the cooling salt is placed in thermal contact via a circulating helium gas type of heat exchanger as described by Keystone, Thoulouze and Lacaze[17]. A schematic diagram of the cryostat is shown on Fig. 2 where the set of dewars providing the 4.2K environment have been omitted.

There are two separate pumping manifolds; one serves mainly to pump over the liquid helium in the 1K plate or pot and is connected to a large Kinney pumping station serving the whole laboratory while the other manifold provides the high vacuum necessary to evacuate the calorimeter chamber and the gas heat exchanger; it has facilities to introduce metered amounts of exchange gases (H_2 or He) and is used in various stages of leak detection.

This cryostat including the high vacuum manifold is mounted on a metal plate attached to an elevator fixed to the laboratory wall. This vertical motion is neeessary to put in place the liquid nitrogen-liquid helium dewar set that rests on the floor.

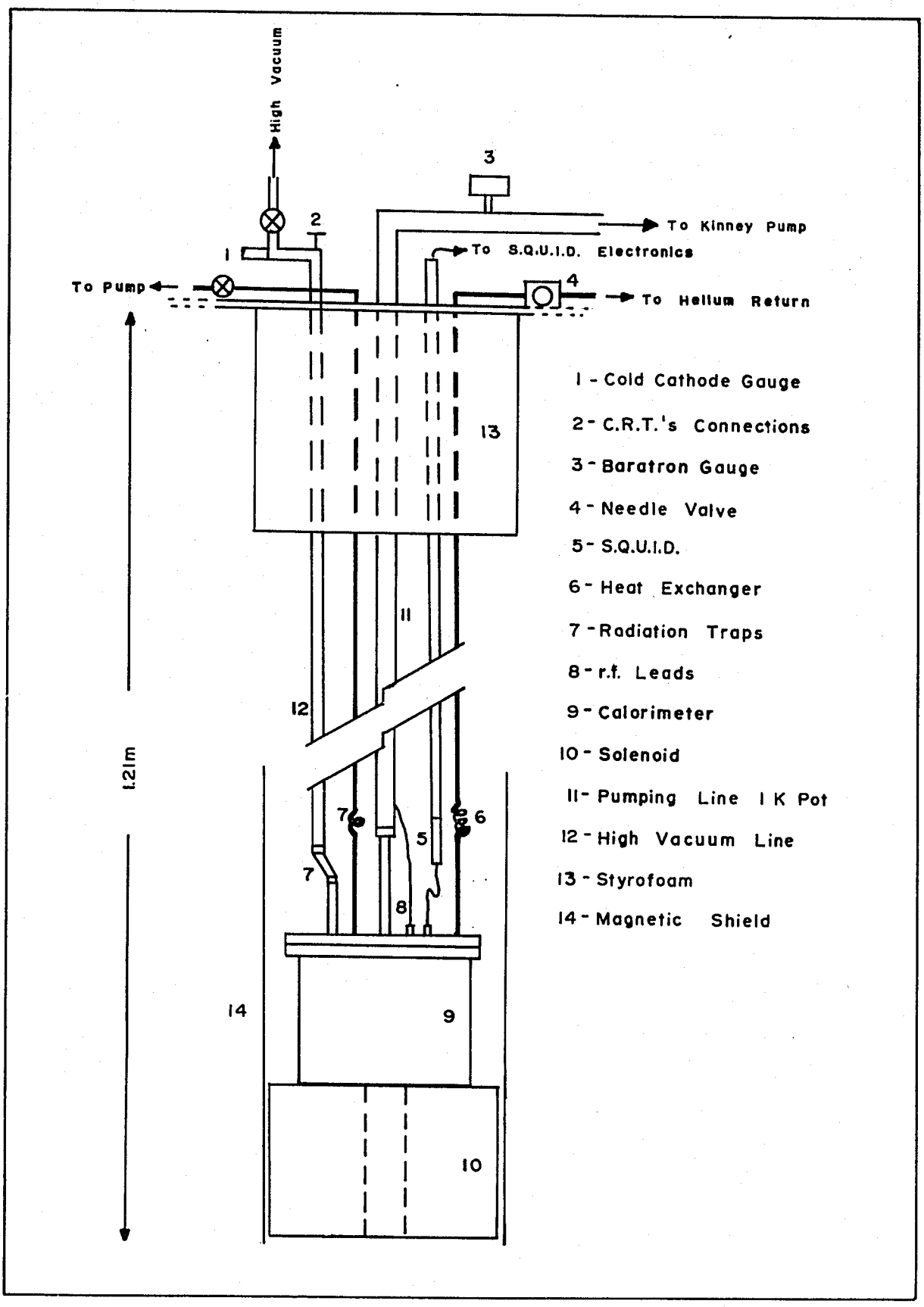

Fig. #2 Schematic Diagram of Cryostat

To reduce vibration to the cryostat, the pumping line from the 1K plate and the return line from the cryostat were connected to the main return line of the laboratory by a flexible rubber hose.

At the beginning of an experiment liquid helium is syphoned in. As some difficulties were experienced with this set-up, a few remarks on the transfer procedure will be given.

Initially a great deal of difficulty was encountered transferring the liquid helium with any degree of efficiency. The first solution involved taping a deflecting shield to the heat exchanger, and another shield taped to the upper plate of the calorimeter. A twelve-inch extension was soldered to the end of the syphon to ensure that the tip was well below the calorimeter flange to effectively use the full cooling power of the liquid helium and its vapour. For a secondary and any subsequent filling, the extension was removed to prevent excessive boiling on retransferring which occurs when the warm helium gas comes through at first.

Although the technique did work most of the time, the system was crude and cumbersome to attach each time, since the shields had to be positioned exactly or else the syphon would catch on the upper plate and could not be lowered any further. The liquid helium would then spray on to the upper plate of the calorimeter and be

directed up and out of the dewar resulting in a waste of liquid helium. This system was later abandoned for a more reliable guide.

A 9.6 mm O.D. by 61 cm long stainless steel tube had a 9.6 mm wide by 40 cm long section removed. The lower end of the slotted tube was then closed to be elliptically shaped. The upper end was flared to fit tightly into the syphon guide. However, after transfer, rapid boil-off was observed through the syphon guide. The reason for this is not clearly understood. In an effort to prevent this from reoccurring, a series of holes, 1.6 mm in diameter, were drilled below the flared part, but this did not stop either the blow-off or the rapid boiling of the liquid helium. The guide tube was then lowered to be approximately 10 mm below the entrance of the syphon guide. The upper part of the slotted tube was attached with masking tape to the pumping line of the 1K refrigerator and the bottom was simply taped to the calorimeter flange to hold it secure.

This guide tube also fills another purpose; it protects the SQUID from thermal shock. During one run, the syphon dislodged the guide on the initial transfer and on the subsequent transfer, the warm gas made the SQUID normal. When it returned to its superconducting state, it was too noisy for the electronics to "lock". It

required eighteen hours to return to its original placid state.

APPARATUS

We will discuss in turn nine of the main components of the cryostat, they are: (1) dewars, (2) 4.2K environment, (3) 1.3K refrigerator, (4) experimental stage, (5) salt pill, (6) gas heat exchanger, (7) Carbon Resistance Thermometers, (8) N.M.R. head, (9) solenoids and magnetic shielding.

(1) Dewars

The experiment was performed in a set of stainless steel dewars. The nitrogen dewar is 19.9 cm I.D., 25.3 cm O.D., and 119.7 cm deep and was manufactured in house to replace the original stainless steel dewars. The outer wall of the dewar is formed from a rolled sheet of stainless steel and the inner wall is an 8 in. stainless steel tube. Wrapped around the outside of this tube are several layers of aluminized one half mil mylar. A charcoal trap was anchored to the bottom plate. The helium dewar, 13.9 cm I.D., 16.6 cm O.D. and 122 cm deep, was also manufactured in house. The inner wall is a 5½ in. stainless steel tube specially manufactured for cryogenics as it had been annealed after forming to prevent deformation on cooling. The problem of the deformation plagued the original helium dewar. As with the nitrogen dewar, the

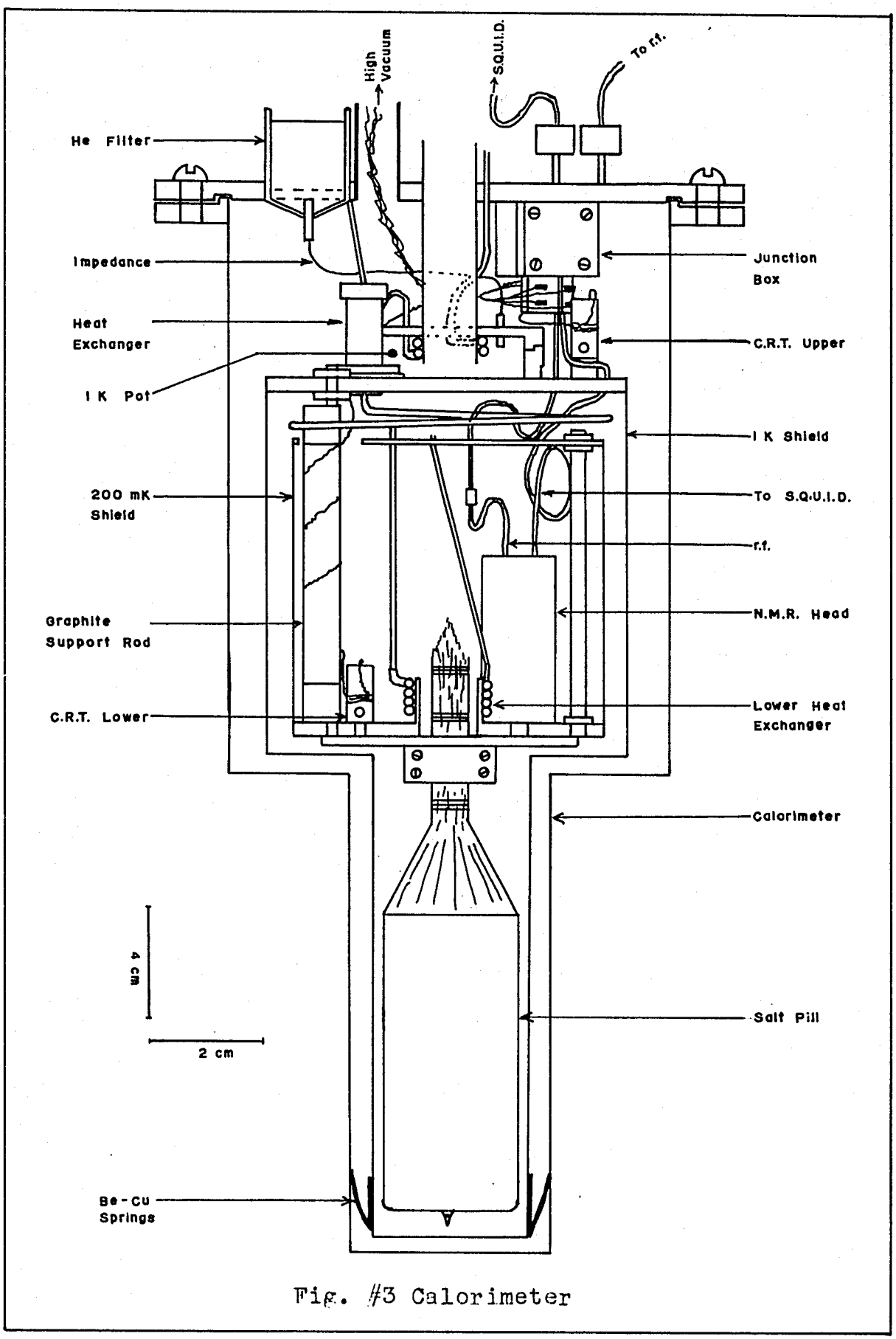

Fig. #3 Calorimeter

outside of the tube is wrapped with the aluminized mylar. Since the SQUID is extremely sensitive to mechanical vibrations, it is necessary to minimize the agitation caused by boiling by using the aluminized mylar to reduce the heat input to the liquid nitrogen and liquid helium.

The helium dewar is sealed at the top by a stainless steel flange and by a rubber "o" ring. Heat transfer down this dewar is reduced by a styrofoam plug.

(2) 4.2K Environment

Since the critical current of the SQUID is temperature dependent, it must be kept in the liquid helium at 4.2K. The means that the bath cannot be pumped on and, therefore, this necessitates a refrigerator to cool the salt pill to 1K prior to demagnetizing and a high vacuum system to thermally isolate it.

The inner part of the experiment is protected from the 4.2K by a copper calorimeter. The calorimeter can, has, at the top, a brass flange that has been drilled and tapped for 8-32 brass bolts. The can is bolted to a matching upper flange consisting of a brass plate through which the various tubes and wires pass connecting the experiment to the outside environment. Originally, all the seams of the calorimeter can had been soft soldered. However, these joins developed leaks as they could not tolerate the strain imposed by the banging of the superconducting solenoid whichhad a tendency to sway when the

entire apparatus was lowered into the dewar. The flange on the calorimeter can had to be silver soldered to ensure a strong leak tight joint.

Indium metal wire is used to seal the calorimeter can to the upper plate. This is done by first cleaning the two brass surfaces to remove any grease, dust or hair. The indium wire (thirty to forty mil in diameter) is coated with a thin film of Apiezon N grease. The grease, which serves as a release agent, is found useful to remove the crushed indium wire after opening the calorimeter since the indium forms an alloy with the brass and cannot be easily removed. The grease on the wire does not have any detrimental effect on the sealing properties of the wire. In over thirty experiments, only one leak attributable to the wire was detected.

(3) 1.3K Refrigerator and Shield

The design of the 1K refrigerator is essentially that of De Long, Symko and Wheatley[16], consisting of a filter, an impedance, an evaporating chamber, a pumping line and the necessary external pump.

The filter which is necessary to avoid any dust from entering the impedance line, is a sintered brass plug (a General Motors type gas filter) mounted in a close-fitting brass sleeve located on the upper plate of the calorimeter.

The original impedance consisted of a simple,

small, internal bore capillary. With it, the lowest temperature that could be achieved at the maximum pumping speed available was 1.6K. This is not a good enough initial temperature for efficient magnetic cooling.

This capillary was partially removed and a new impedance installed. This new impedance is a stainless steel capillary (0.25 mm I.D. by 18 cm long) with a 0.25 mm by 15 cm long Nichrome wire pushed through. Since the measured clearance between the wire and the wall of the capillary is essentially nil in all cases, a high impedance was expected. The manufacturing of the impedance is quite simple. The capillary was reemed out with a 0.20 mm Nichrome wire. This removed most of the dirt and smoothed out any burrs that were present. A stream of water was blown through, followed by a rinsing of acetone to clean the bore. The capillary was then air dried. The wire to be inserted as the restriction, was wiped clean with a paper towel, rinsed with acetone and allowed to dry. The wire was then pushed into the capillary. If the wire did not slide in all the way because the surface of it was nicked or scored, it was smoothed with 2/0 emery paper until it did fit.

Following the procedure of De Long et al.[16], the impedance factor, Z, of the capillary was measured, where Z is defined by

$$Z = \frac{1}{\eta} \frac{\Delta P}{\forall} \qquad (29)$$

Where η is the coefficient of viscosity of the gas, ΔP is the pressure drop across the impedance for a volume flow rate $\forall$. As the η of air is almost equal to that of helium at room temperature, air was used to measure Z.

To actually measure Z, the flow rate through the capillary, $\forall$, was measured with a bubble type, horizontal flow meter. The flow meter consisted of a plastic T junction: to one side was attached the impedance to be

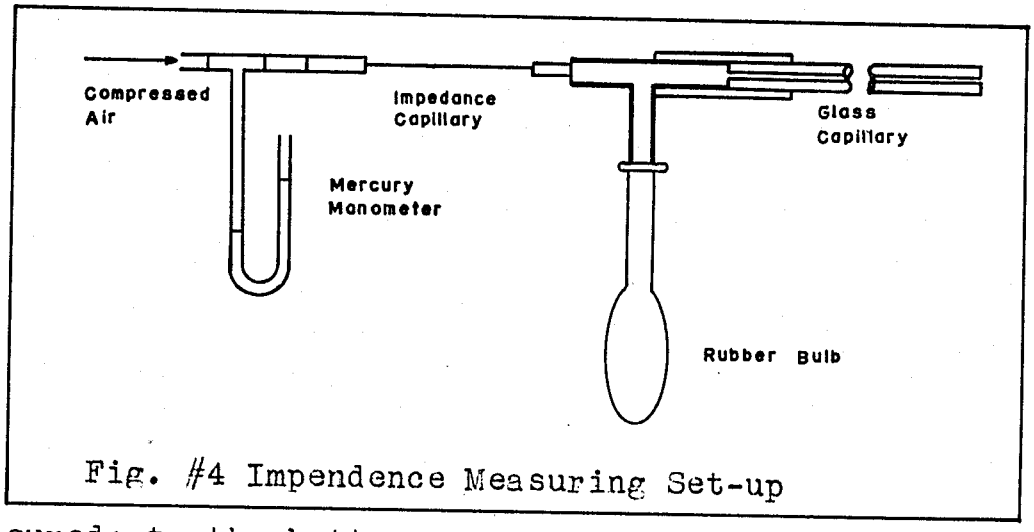

Fig. #4 Impendence Measuring Set-up

measured; to the bottom, a rubber bulb containing "Snoop"; and to the other side of the T, a 1 mm I.D. by 20 cm long glass capillary. Prior to measuring the impedance, the bore of the capillary was wetted with "Snoop" to reduce the friction of the bead of "Snoop" as it moved along the tube. This bead was timed as it moved between two fixed points. An average of several readings was taken as the times were quite varied (approx. 10%).

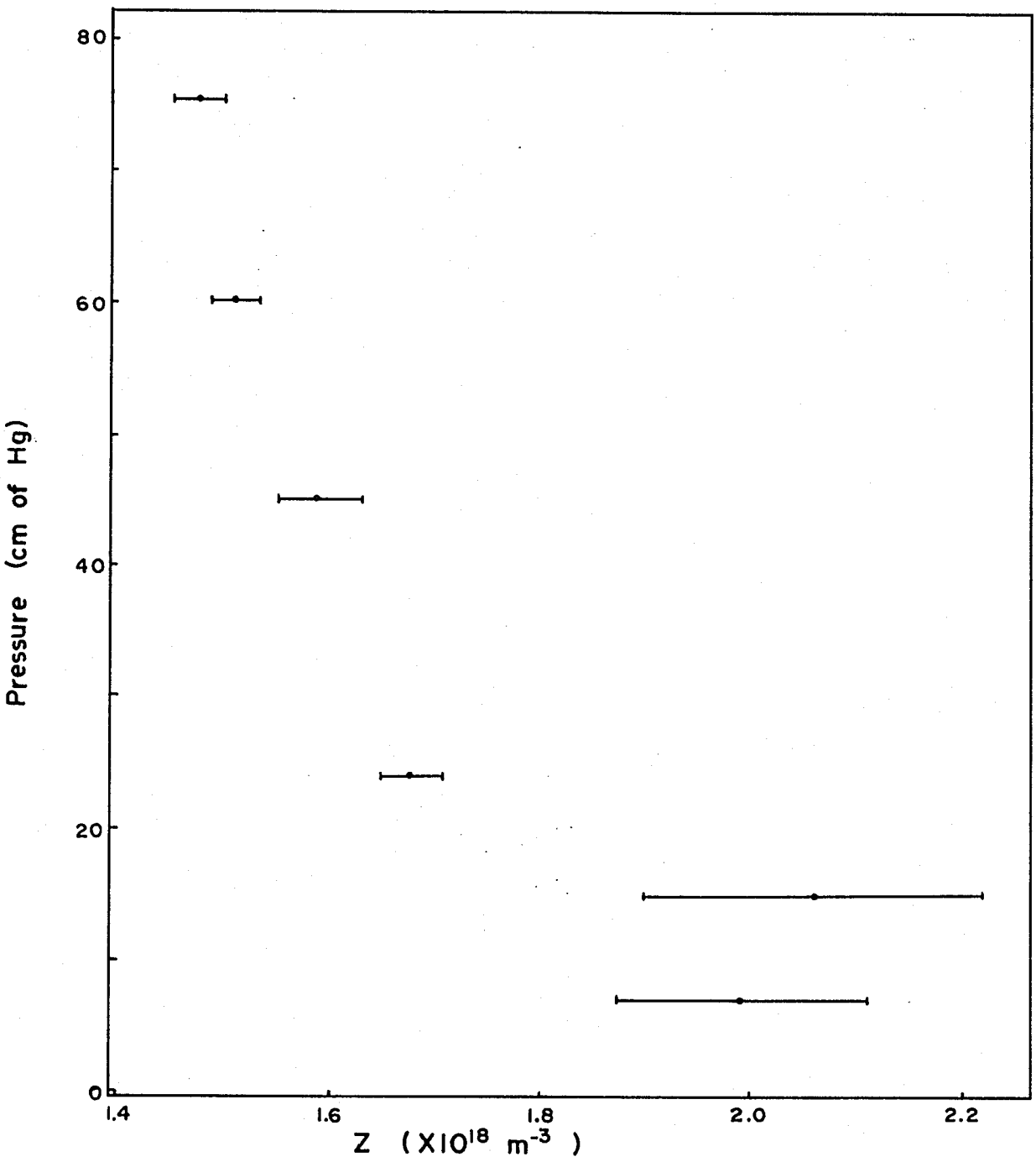

Fig. #5 Variation of Z With Pressure

Different wires were tried until the correct impedance was found.

The value found for Z is 1.4×10^{18} m^{-3}. This compares to the values of De Long et al. who had found that Z should be between 0.67 to 2.0×10^{18} m^{-3} to achieve a temperature of 1.3K. The value of Z, 1.4×10^{18} m^{-3}, was the minimum value obtained, since it was found that Z is dependent on ΔP. The range of values for Z, as a function of ΔP, was between 1.4 to 2.0×10^{18} m^{-3}.

The evaporating chamber, which has an interior surface area of 25 cm^2, and thus the temperature of the plate will be within 1% of the liquid helium[18], is constructed of a copper plate (10.1 cm by 3.3 mm thick) to which is soldered a copper cap (See Fig. #3). Coming in through the top of the cap are the input and the output of the heat exchanger, the impedance capillary and the pumping line made of 9.5 mm O.D. stainless steel that enters 1.0 cm into the chamber. The tubing of the heat exchanger is wrapped around the end of the pumping line and soldered to it to ensure good thermal contact.

The entire refrigerator and lower stage, which is fixed to the 1K plate by three graphite rods, are all supported by the stainless steel pumping line of the 1K plate. The plate is used to thermally anchor, at 1K, all the electrical leads going to the lower stage.

Mounted on the plate is a carbon resistance thermometer (described below) to monitor the temperature and hence the performance of the refrigerator, and a small second heat exchanger.

The pumping line of the refrigerator is directly connected to the head of the cryostat by a series of successively larger bore stainless steel tubes and includes a radiation trap.

The pressure in the line at the top of the cryostat is measured with either a mercury manometer or an MKS Baratron gauge (type 170M). The accuracy and the four digit display of the Baratron permit an easy check on the functioning of the 1K plate. Once the temperature of the plate has stabilized, as measured by the carbon resistance thermometer, the operating pressure is steady and in the order of 1.1 to 1.2 mm of Hg. Any sudden heat load on the pot would cause the pressure to increase to typically 1.6 to 1.9 mm of Hg (eg., when the salt is warmed as the superconducting solenoid is energized). Monitoring the carbon resistance thermometer is no longer necessary unless an accurate reading of the temperature is required.

The pumping line from the head of the cryostat is connected to the control vacuum manifold of the laboratory by a flexible rubber hose. This hose is used to reduce the vibration to the experiment which would normally disturb the SQUID operation and introduce an unacceptable heat leak to

the salt. The pump for this system is a Kinney (type KDH 130) with a pumping speed of 60 l s^{-1}.

A copper shield completely surrounds the lower stage and the salt pill. It is securely attached to the 1K plate by three screws (00-72) which also improve the thermal anchoring of the shield to the refrigerator. Since the 1K plate and lower stage are supported by just the pumping line, the entire structure forms a pendulum. To reduce any vibrations of this form, four beryllium copper springs were attached with masking tape to the bottom of the "tail" of the 1K shield. These springs were formed by bending back a piece of beryllium copper to an angle of 30° and then the end wrapped with TPFE tape to reduce friction when the calorimeter can is installed.

(4) The Experimental Stage

The experimental stage is essentially a copper plate 52.6 mm in diameter by 5.0 mm thick which has a heat exchanger in the center, the NMR head and two carbon resistance thermometers (all will be seen later) (See Fig. # 3). Mounted below the plate is the salt pill to supply the magnetic cooling for below 1K. The salt pill will be described later.

The experimental stage is supported by three graphite rods (AGOT graphite, 6.3 mm in diameter 11.0 cm long) located at the edge of the plate. These rods replace three stainless steel supports since a calculation showed

that too much heat was being conducted down the original stainless steel support rods. One end of a delrin rod was machined to form a sleeve (6.3 mm in diameter by 10 mm high) that would fit over the end of the graphite rod. In order for the graphite rods to fit the original holes in the experimental stage and 1K plate for the stainless steel supports and not to touch the 200 mK shield, the threaded section had to be exocentrically located. It was hoped that the delrin, being more flexible than the rigid graphite, would prevent the graphite from breaking. However, this flexibility allows the lower stage to vibrate, causing a noisy signal to the SQUID. The graphite also serves as an effective adsorption pump[12] to remove any traces of helium gas in the calorimeter chamber.

Shielding of the experiment is provided by two copper shields. The upper shield is a copper disc that is anchored to the experimental stage by three copper rods (2.5 mm in diameter by 10.5 cm long). The plate is drilled to allow the graphite support rods through as well as all the electrical leads and the heat exchanger capillary. The other shield is a thin walled copper tube (53.8 mm in diameter, 0.6 mm thick and 103.3 mm long) that surrounds the experimental area. This tube is held in place by three small screws (00-72), that allow the

shield to be removed for work to be done on the experiment. When installed, the sleeve thermally short circuits the experimental stage to the upper shield.

To prevent the lower stage from vibrating, three strips of mylar (3 cm long by 6 mm wide by 0.13 mm thick) were coiled and one inserted in each of the spaces between the graphite rods and the upper shield (See Fig. #3). This did improve the signal to noise ratio appreciably.

(5) Salt Pill

The salt pill consists of 53 g (0.11 g of ion) of chromium potassium alum crystallized onto a bundle of 620 silver wires (0.25 mm in diameter)[17]. The spacing of the wire bundle is maintained by a plastic screen between each successive layer of wire. Since the salt dehydrates rapidly, it is protected by a thin coating of Silicone grease and a layer of plastic wrap. To reduce the heating caused by radiation, the pill is wrapped in $\frac{1}{2}$ mil aluminized mylar. Two nylon spacers are used to prevent the pill from touching the 1K shield.

The holder for the wire bundle was machined from a solid copper disc to form a clamp with a detachable side. The bundle is pushed through the hole in the center of the holder and clamped into position. The holder is then mounted underneath the experimental plate by three brass screws (8-32). A thin film of Apiezon N grease is used

to ensure good thermal contact between the holder and the experimental stage.

(6) Heat Exchangers

The circulation of helium gas through four heat exchangers is used to cool the experimental stage and the salt pill from 9K to 1.3K prior to demagnetizing (See Fig. #3).

The first exchanger cools the gas to 4.2K. It is just a spiral of copper tubing (2.4 mm O.D. by 0.8 mm I.D. by 33 cm long) located in the bath just above the flange of the calorimeter. The second heat exchanger at 1.3K, is a coil of copper tubing (2.4 mm O.D. by 0.8 mm I.D. by 5.4 cm long) and is soldered to the pumping line inside the 1K refrigerator. The third is also a coil of copper tubing (2.4 mm O.D. by 0.8 mm I.D. by 2.4 cm long) soft soldered to a hollow cylinder of copper on the experimental stage. It cools the stage and salt pill to 1.3K.

To minimize the heat leak down the return capillary from the heat exchanger on the experimental stage, it was necessary to obtain adequate thermal anchoring to the 1K plate. As the normal heat load during cooling, on the 1K plate is less than its critical power level, the plate remains at its normal operating temperature. By allowing a small volume of helium to condense in the exchangers, superfluid creep can be used to cool the lower stage to 1.3K without pumping to circulate the gas[17]. By employing

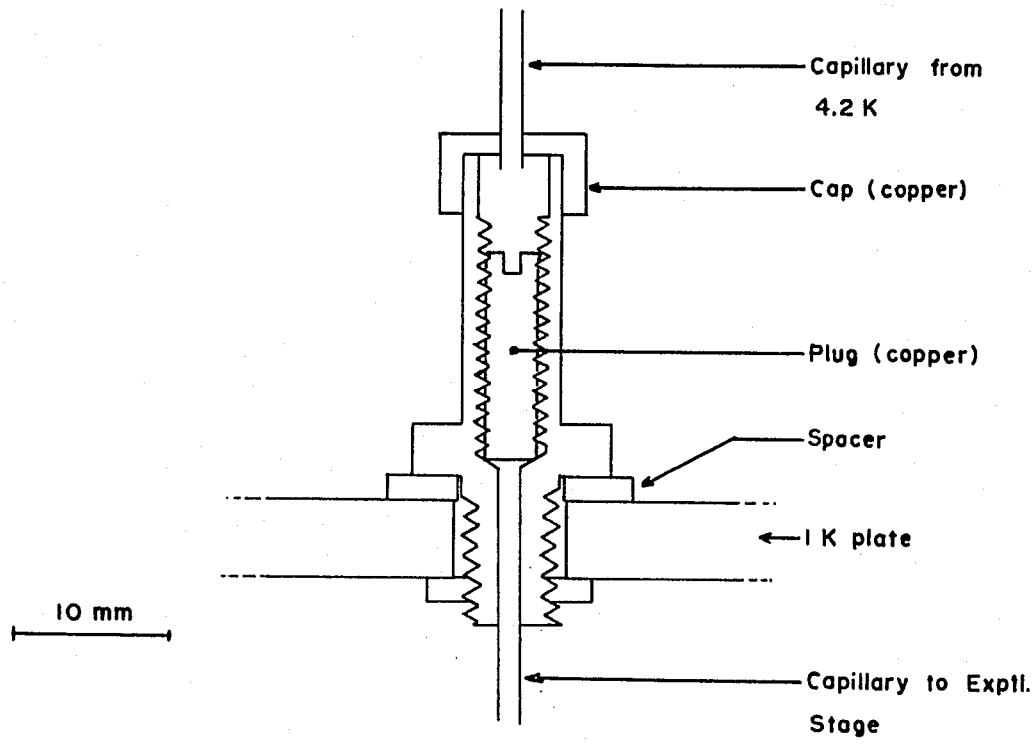

Fig. #6 Heat Exchanger

two exchangers at 1K instead of only one, it would be possible then to obtain cooling along both capillaries. Due to restrictions in space, this second exchanger had to be quite small. It was machined from a piece of copper stock that was drilled and tapped with a 10-24 thread (See Fig. #6). A solid copper plug (4.36 mm in diameter) with a notch at the top, was cut for the 24 thread but the cut was only 8 mil deep; it was then tightly screwed into the first piece. This leaves a triangular path of 18 cm in length and contact area of 2.4 cm^2 through the gap in the thread for the gas to follow. The gas is cooled equally on all three sides of the triangle, as the plug is in thermal equilibrium at all times with the rest of the exchanger[12].

The two exchangers at 1K are connected to the experimental stage by two stainless steel capillaries (1 mm O.D., 0.75 mm I.D., 30 cm long). This length was chosen to reduce the heat leak down the length of the capillary.

Helium gas, taken from the gas evaporating from the bath and passed through a charcoal trap at 77K, is pumped by a Sargent Welch pump (Model #8805, 0.83 ls^{-1}) through the exchangers at a rate that can be controlled by a needle valve at the intake.

(7) Carbon Resistance Thermometers (C.R.T.)

To measure the temperature, Speer resistors

(1002 grade, 220Ω nominal room temperature value) were used following the recommendation of Johnson (cf. Johnson and his references).

The leads of the resistors were trimmed to leave a short extension of 3 mm and then the resistor was ground flat to form a platelet 0.3 mm thick. In grinding, most of the tin-lead solder was removed from the leads, improving the thermal contact between the resistor and the wire leads . The wire leads were #46 AWG copper wire and were soldered to the resistor with Indalloy solder. The resistors were wrapped in a 1 mil mylar sheet that had been smeared with Apiezon M grease to improve thermal contact. The carbon element thus prepared, was sandwiched between two conically shaped half cylinders, wedged into the tapered hole of a cylindrical holder, secured in place by a threaded section. The support was made of copper and then gold plated to ensure good, permanent thermal contact properties. These units give excellent response to temperature changes; any variation in pumping on the 1K plate would result in an immediate change of the resistor.

The resistances of the thermometers were measured to within 0.1% with a three wire 87 Hz Wheatstone bridge using phase sensitive detection. The bridge was previously constructed in the lab and consisted of General Radio 510 decades, GR 500J 10KΩ (± 0.025%) fixed standards, a

Princeton Applied Research model 129 Phase Sensitive Detector (P.S.D.), a Hewlett Packard model 651A test oscillator and a Philips strip chart recorder. The bridge is a more refined version of the one used by Johnson[19]. Ground loop problems, capacitive effects, pick up and vibration have been virtually eliminated by enclosing all components in a strong steel box, and by having a single ground post for all connections (the amphenol connectors were attached to sheets of phenolic, leaving the grounds floating). (See Fig. # 10)

The resistors were individually calibrated from 4.2K to 1.35K against the 1958 Helium Temperature Scale by immersing the resistors in the helium bath directly and pumping on the bath. The pressure was measured with a mercury manometer connected to the bath at the head of the cryostat. For pressure below 10 cm of Hg, the MKS Baratron gauge was used. Agreement between the manometer and the Baratron gauge was within 2% in the overlapping range (<1mK). A germanium resistor, Cryocal model #CR 1000-1.5-100 (range 1.5K to 100K) was used as a check. Small discrepancies between the temperature measured by the manometer and that of the germanium resistor appeared, but the difference is believed to be from a change in the calibration of the germanium resistor through aging.

For calibration of the lower C.R.T. below 1.4K,

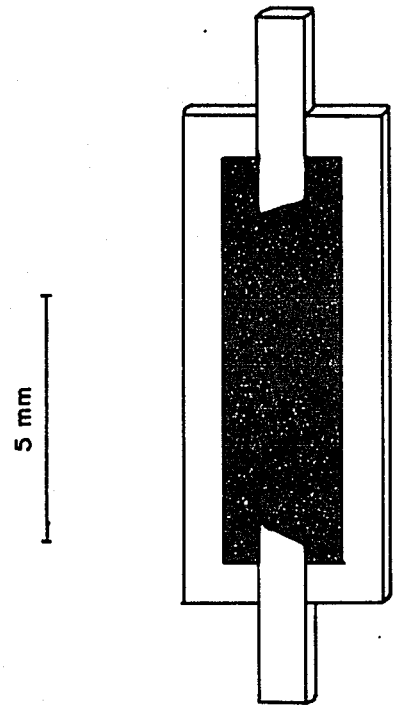

Fig. #7 Resistor Platelet

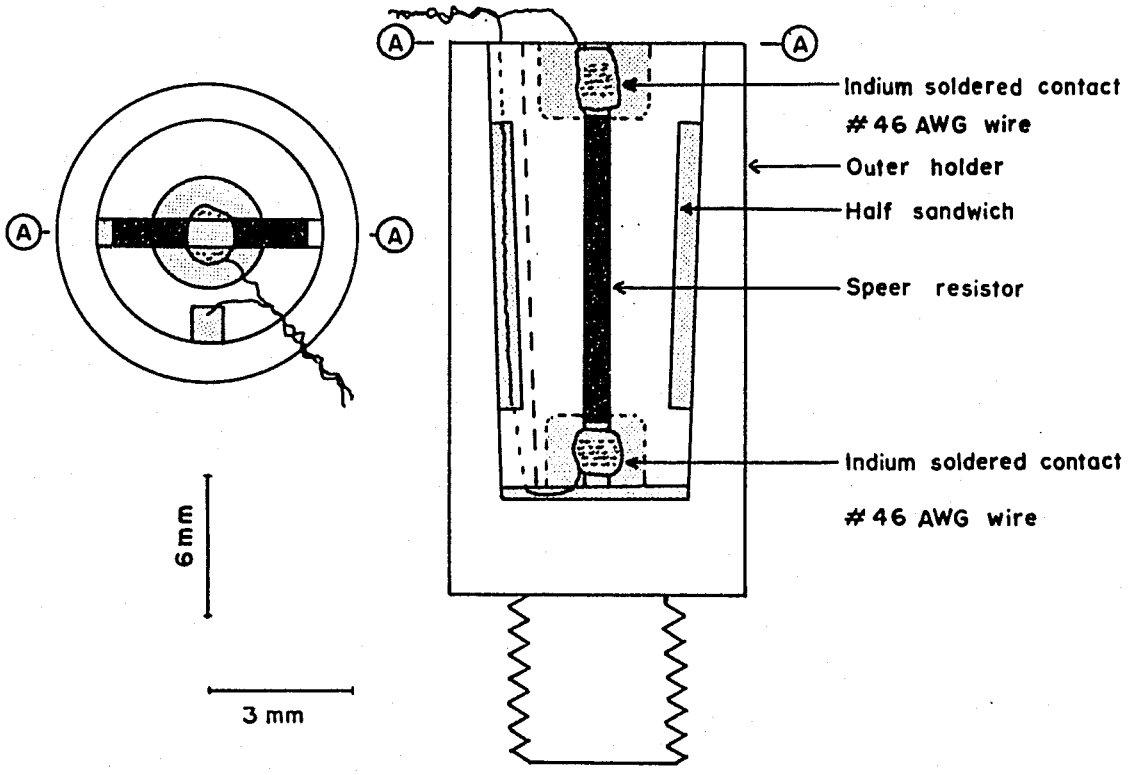

Fig. #8 Carbon Resistor Thermometer Assembly

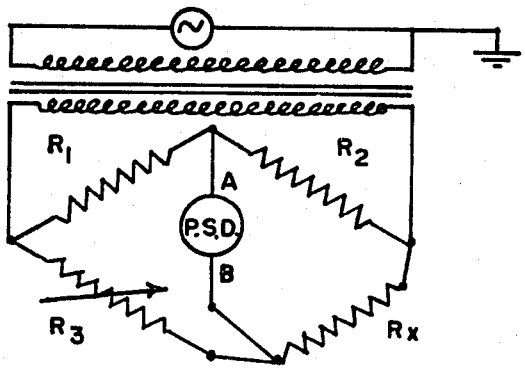

Fig. #9 Schematic of Resistance Bridge

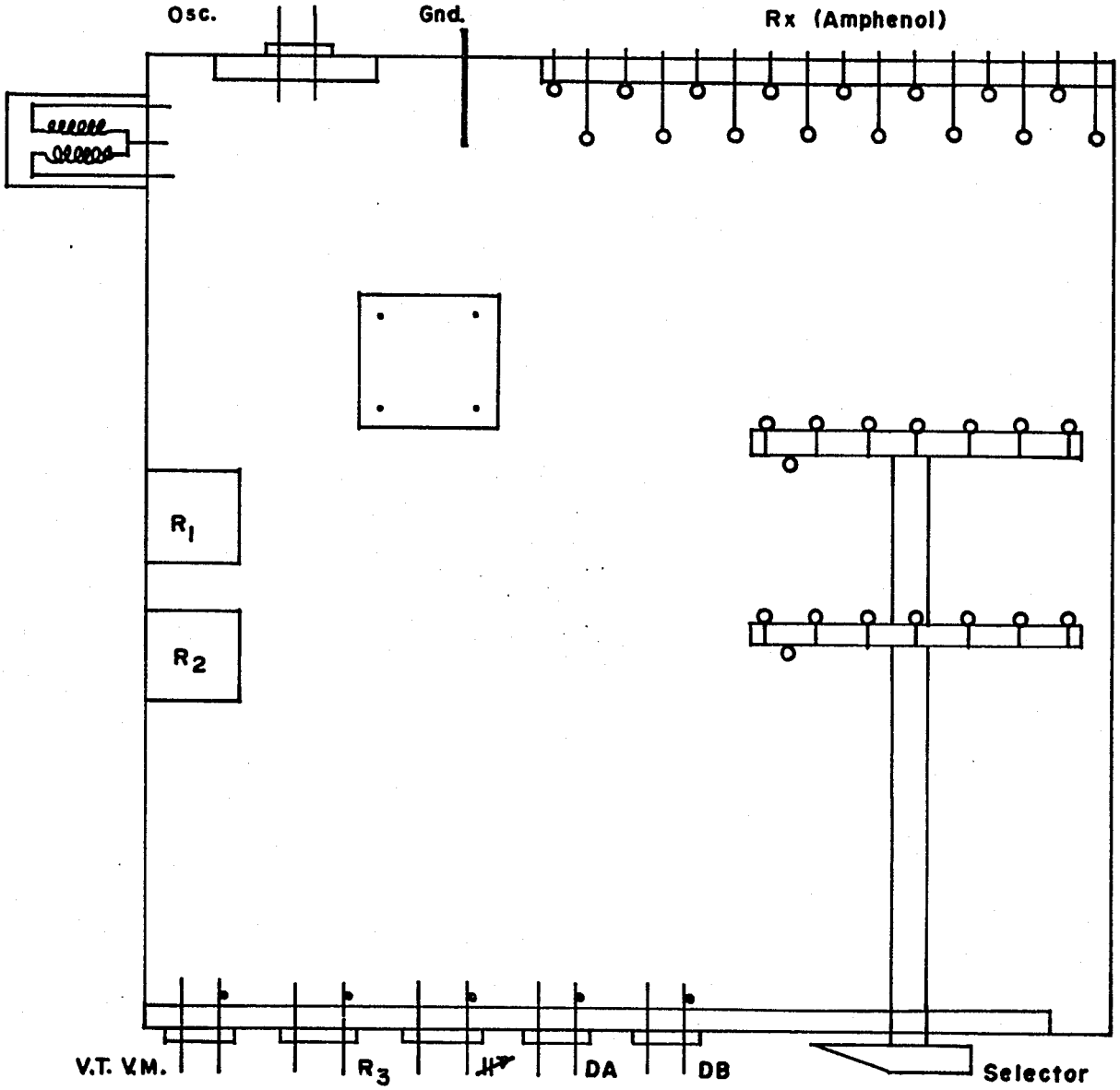

Fig. #10 Wiring Diagram of Bridge

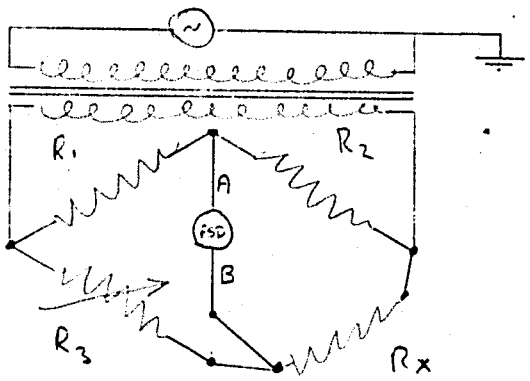

Fig # A.C Wheatstone Bridge

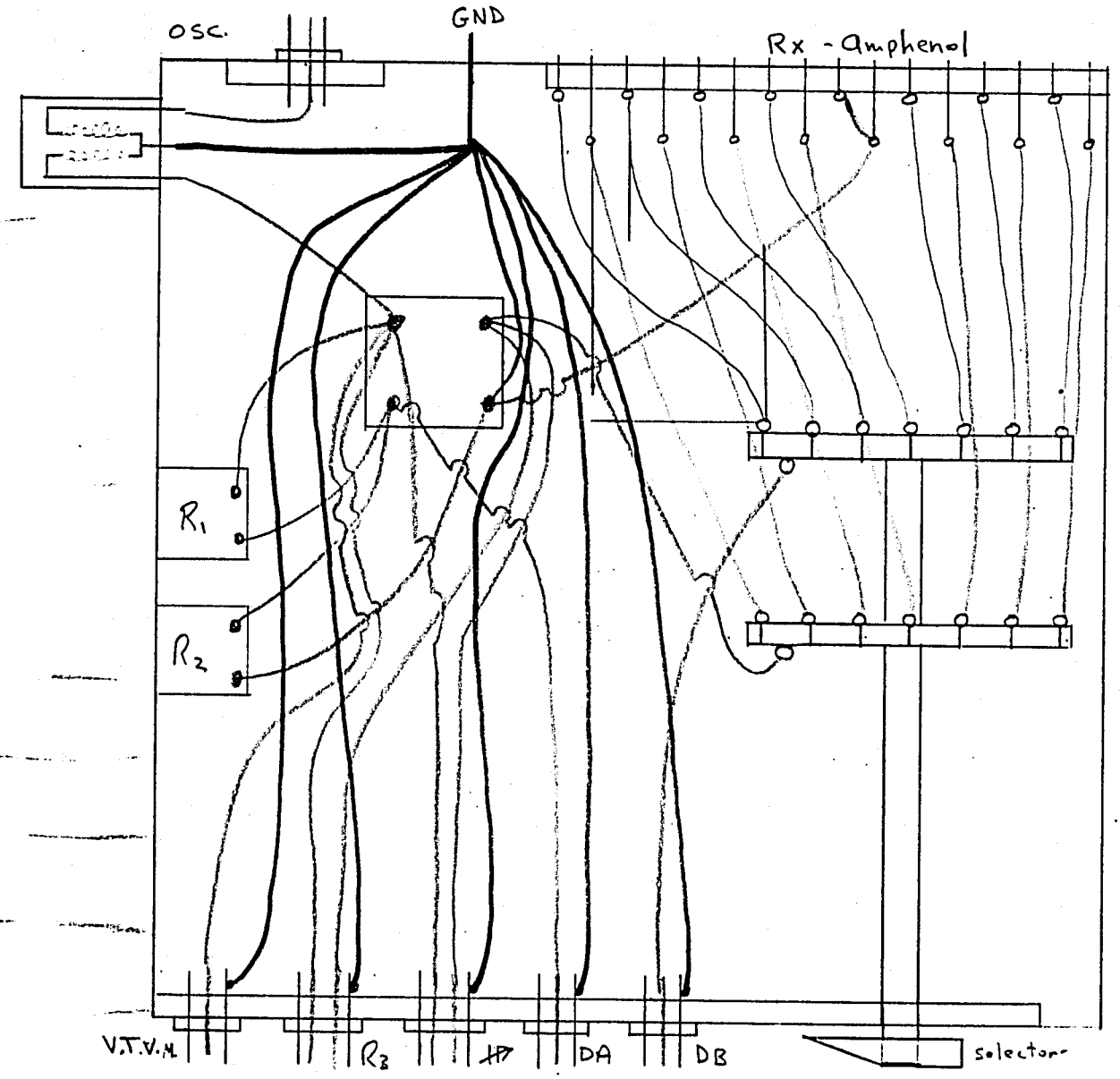

Fig # Circuit Diagram of A.C. Bridge

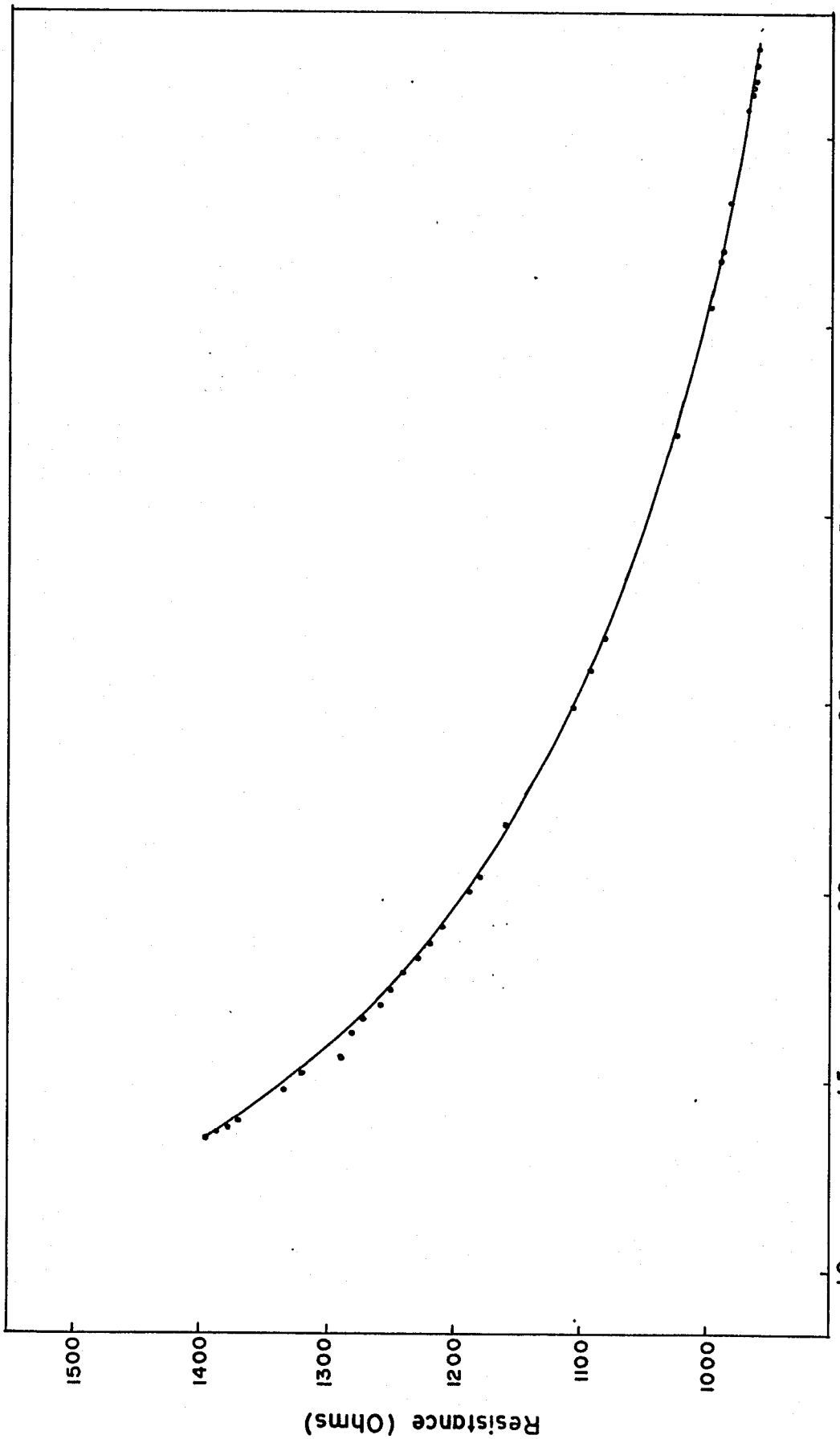

Fig. #11 Calibration Curve R_{upper}

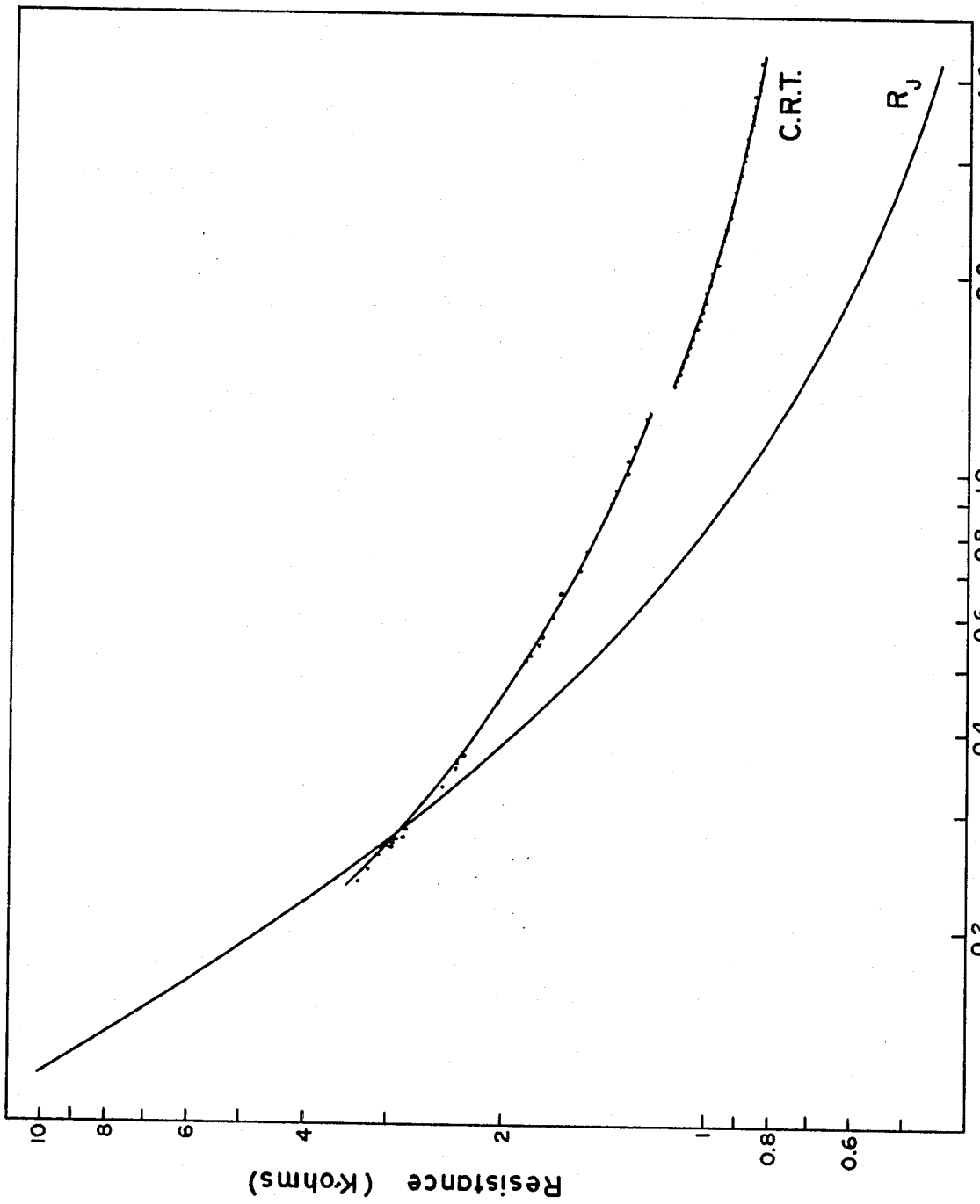

Fig. #12 Calibration Curve R_{lower}

the C.R.T. (R_j) used by Johnson[19] was mounted beside the lower C.R.T. on the experimental stage. R_j had been calibrated to 80 mK, but six years ago. It is not known what effect age has on Speer resistors, so as a check, the calibration was carried from 200 mK to 2K to compare with the previous calibration. The two lines do not quite match exactly, but the accuracy is adequate for the proposed usage for this set of experiments.

The graphs for the calibration are on pages 42 and 43. Johnson's calibration is included to show the much slower rise of resistance at lower temperatures, probably due to the geometry of the resistors, R_j being cylindrical with only the insulation removed versus the platelet form described above for our C.R.T. A least squares fit was done for the C.R.T. using the expression of Hetzler and Watson.[20]

$$\frac{1}{T} = A - BR - CR^{\frac{1}{2}} \qquad (30)$$

The solid line drawn through the points represents the above expression. The values for the constants A, B, and C are included in the tables.

In attempting a calibration of the lower resistor against R_j, a great deal of difficulty was encountered due to time wasted trying to rebalance the bridge for each measurement. A relationship between the off balance voltage of the P.D.S. null detection and the resistance was sought.

From Halliday and Resnick[21], the current, i, through a galvanometer of a Wheatstone bridge is given by

$$i = \frac{E\,(R_s - R_x)}{(R + 2R_g)\,(R_s + R_x) + 2R_s\,R_x} \qquad (31)$$

where R_s is the resistance of the standard decade resistors, R the standard resistors (10KΩ ± 0.025%), R_x the unknown resistance, and R_g the resistance of the galvanometer, here the P.S.D.

$$i\,R_g = V = \frac{E\,R_g\,(R_s - R_x)}{(R + 2R_g)\,(R_s + R_x) + 2R_s\,R_x} \qquad (32)$$

Now $2R_g \gg R$, and $R_g\,(R_s + R_x) \gg R_s\,R_x$

$$V = \frac{E\,\cancel{R_g}\,(R_s - R_x)}{2\cancel{R_g}\,(R_s + R_x)} = \frac{E\,(R_s - R_x)}{2(R_s + R_x)} \qquad (33)$$

incorporating the amplification of the P.S.D.

$$V_{out} = K\,\frac{(R_s - R_x)}{(R_s + R_x)} \qquad (34)$$

The error in the above expression is estimated to be no worse than 1 part in 2×10^4.

To calibrate, the bridge is balanced initially at any constant temperature to give R_o. Then the bridge is unbalanced by changing the decade resistors to R_1 for a near maximum deflection of the P.S.D. The output, V_{out}, of the P.S.D. may be read with digital voltmeter for better accuracy or recorded on a strip chart recorder.

$$K = V_{out} \frac{(R + R_o)}{(R - R_o)} \qquad (35)$$

K remains constant to within 2% (with a multiplication factor being employed) when changing scales on the P.S.D., allowing rapid measurements to be taken with good precision. However, it was found that K does vary from run to run (approx. 10%), but no real vairation was noticed during any particular run.

(8) N.M.R. Head

In the magnetometer detection of the N.M.R. phenomena used, the sample is exposed to a local r.f. field $B_1 \cos \omega t$, whose frequency is swept through resonance. It is placed in a constant magnetic field, B_o, trapped in a large cylindrical superconducting tube which is perpendicular to B_1. The nuclear magnetization along B_o is monitored by the secondary coil of a superconducting flux transformer whose primary is located in the SQUID element above.

The sample is thus centrally located in what we call the N.M.R. head. The r.f. coil producing the $B_1 \cos \omega t$ field, is wound directly on the sample itself to minimize the required space for it and the magnetometer pick-up coil, and to optimize the filling factor and, therefore, obtain the largest N.M.R. signal possible.

The N.M.R. head is essentially the same as those

used by Goodchild[13], Day[22] and Meredith et al.[14] with some variations to be described below. (See Fig. #13)

The head consisted of four main components (a) the radio frequency shield, (b) pick-up coil of the flux transformer, (c) the field trap and (d) the sample holder and r.f. coil.

(a) The shield (for dimensions, see Fig. #13) was machined from a solid bar of copper stock. Initially the shield had been drilled all the way to the bottom, then the hole was enlarged to 4.8 mm leaving a shoulder for the sample to rest on for accurate positioning, as well as reducing the mass of the shield. The bottom of the shield has been cut to form a hexagon. This permits the shield to be easily tightened to the experimental stage with a small wrench.

(b) The magnetometer pick-up coil, consisting of 20 turns of 76μm insulated niobium wire, was wrapped around the r.f. shield. The middle of the coil was centered on the middle of the sample. To prevent the pick-up coil from shorting to the shield, the shield was first wrapped with a 1 mil mylar sheet.

The twisted leads of the pick-up coil of the flux transformer, were passed through a lead capillary to a brass junction box where it was connected to the leads coming from the primary winding in the SQUID at 4.2K. The junction box was vacuum sealed at the top with Stycast to the underneath

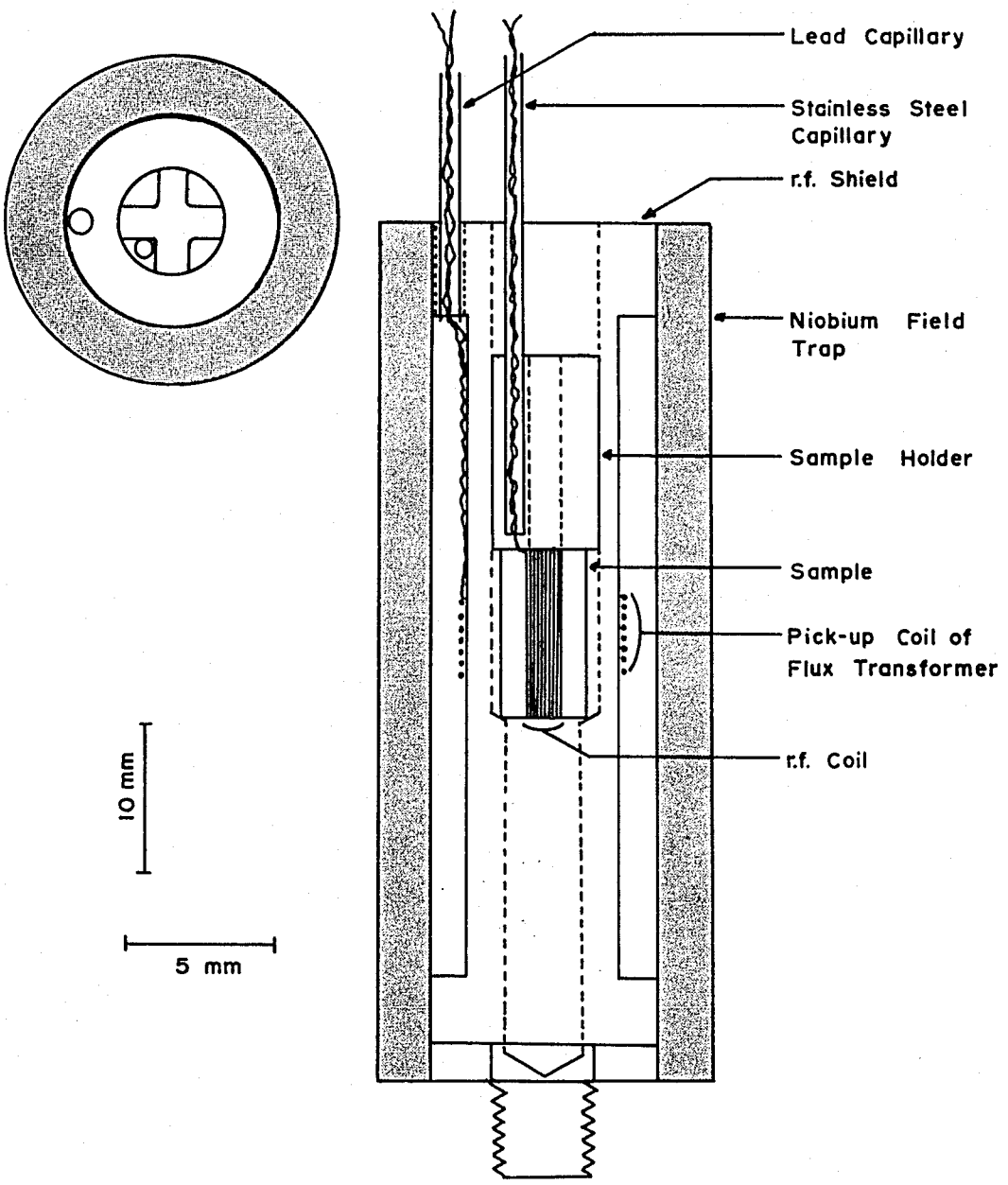

Fig. #13 N.M.R. Head

of the upper flange of the calorimeter. To magnetically shield the circuit at the junction, the box was closed with a coverplate held by four screws and the entire box was wrapped in superconducting lead foil. The leads from the SQUID, shielded by a lead capillary, went through the upper flange of the calorimeter to the junction box. Since the lead capillary could not be soldered to the cap on the upper flange for a vacuum tight seal, an epoxy seal was essential. Stycast was chosen since it has been extensively used to seal wires inside tubing . The Stycast was

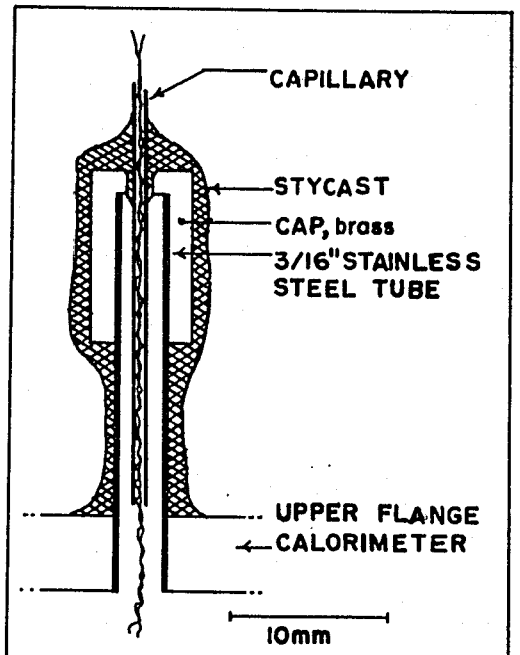

Fig. #14 Stycast Seal

liberally applied around the capillary and cap to avoid any possible channels that may result in leaks. (See Fig. #14) The leads at the SQUID were sealed at the opening of the lead capillary by Stycast and they were also sealed in the

box by Stycast again. Electrical contact between the leads, was made through two small (3.2 mm wide by 7.9 mm long and 3.2 mm thick) niobium blocks set into Stycast to electrically isolate them. The blocks had been drilled and tapped at each end for a small stainless steel screw. The bare lead was pressed onto the niobium block by a washer pressed down by the screw. This type of contact where the leads and the niobium block are cleaned, is as reliable as spot welding and more convenient to use particularly when changing the N.M.R. head for a new sample.

(c) The field trap was a hollow cylinder that had been machined from a round bar of unannealed niobium. The dimensions (12.7 mm O.D. by 9.6 mm I.D. by 57.7 mm long) were chosen to give a snug fit when mounted over the r.f. shield. This close fit was needed to minimize any stray r.f. from leaking around the seams to the pick up coil[12].

To prevent the trap from vibrating, the base of it is smeared with grease that freezes the trap to the experimental stage at lower temperatures.

(d) The sample holder is a small piece of delrin machined in the form of an X. A stainless steel capillary, 50 mm long, is glued in one of the grooves. The r.f. coil, used to induce the nuclear magnetic resonance, is wrapped directly onto the sample. For conducting samples, eg. aluminum, a layer of 1 mil mylar is first wrapped around. The coil consists of 15 turns of #40 AWG wire. The

twisted leads are brought through the stainless steel capillary, and the sample glued to the bottom of the holder.

The sample is then lowered into the r.f. shield; for samples that need not be saved, Araldite was poured in to improve thermal contact, if the sample was to be saved, then Apiezon N grease was used.

The r.f. leads were brought out of the calorimeter through a long stainless steel capillary. The capillary was sealed at both ends with Stycast. As in the case of the lead capillary from the SQUID, the stainless steel capillary could not be soldered to the flange. This meant that Stycast had to be used to seal the capillary to the cap on the upper flange. (See Fig. #14)

The electrical connections between the r.f. leads out of the capillary and a small diameter coaxial cable leading out of the cryostat were insulated and wrapped with copper foil to reduce possible r.f. leakage.

(9) Solenoids and Superconducting Shield

The superconducting solenoid used in the adiabatic demagnetization of the salt is a Ferranti-Packard type 7001-7012-C with a maximum field of 7.0T at 49 amps. The bore of the solenoid is 35.6 mm with a homogeneity of 1%. The solenoid is supported by three stainless steel tubes that are anchored to the head of the cryostat.

The power supply used to energize the magnet is a Hewlett-Packard Harrison 6260A DC Power Supply which is capable of producing one kilowatt (100 amps at 10 volts) and is extremely stable. The current through the solenoid is monitored by measuring the voltage across a standard manganin resistor (50mV = 100 amps) with a D.V.M. During a run, the power supply continually supplies current; the persistent mode of the solenoid is not used.

To minimize eddy current heating on demagnetizing, the current limiting resistor of the power supply is gradually brought to zero by a motorized drive. Time taken for demagnetizing is approximately 30 minutes.

For magnetic shielding, a superconducting lead sheet completely encloses the SQUID, superconducting solenoid and calorimeter. The shield is made from a 1.4 mm thick lead sheet wrapped around an aluminum tube. The seam of lead was soldered together for good electrical contact. The shield has an inner diameter of 127 mm and is 610 mm high.

Supplying the field, B_o, for the N.M.R. field trap is a Helmholtz pair of coils. The coils have a bore of 278 mm and a coil diameter of approximately 380 mm. This large bore allows the dewar set to be located inside the coils. The field factor (calculated) is 1.18mT/amp.

The pair of coils is supported by four aluminum legs adjusted to have the N.M.R. field trap in the centre of applied field.

The power supply is an Eastern Scientific Instrument, capable of 2.25 kilowatts (15 amps at 150 volts). The stability of the power supply is not critical since the supply is turned off once the field is trapped.

The field profile of the Helmholtz pair was mapped with an R.F.L. Industries Gaussmeter model 505 (Hall effect probe) to within 2%. The field profiles are plotted on pages 54, 55 as a function of B along the Z axis and along the X axis.

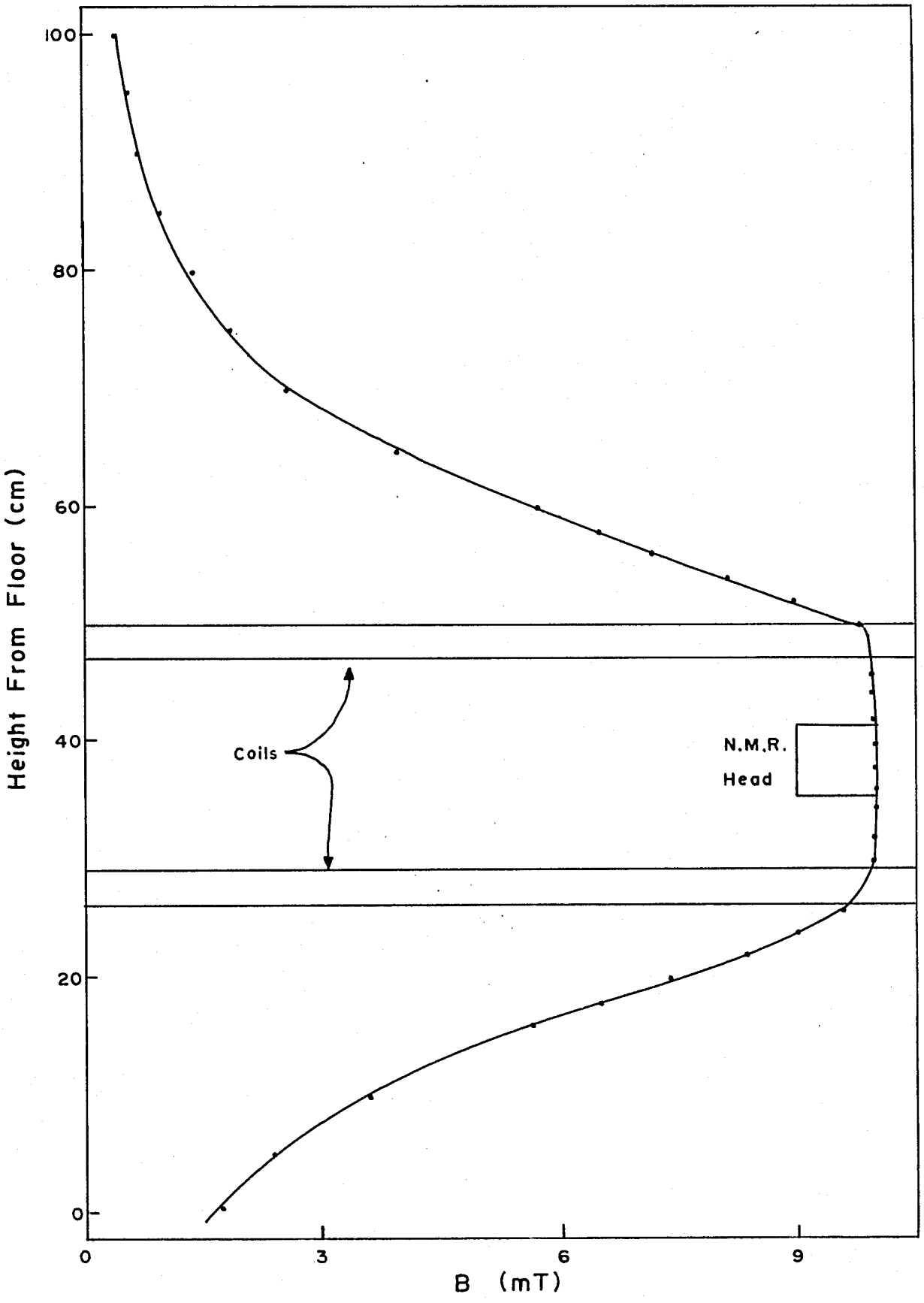

Fig. #15 Field Profile (Vertical) of Helmholtz Pair

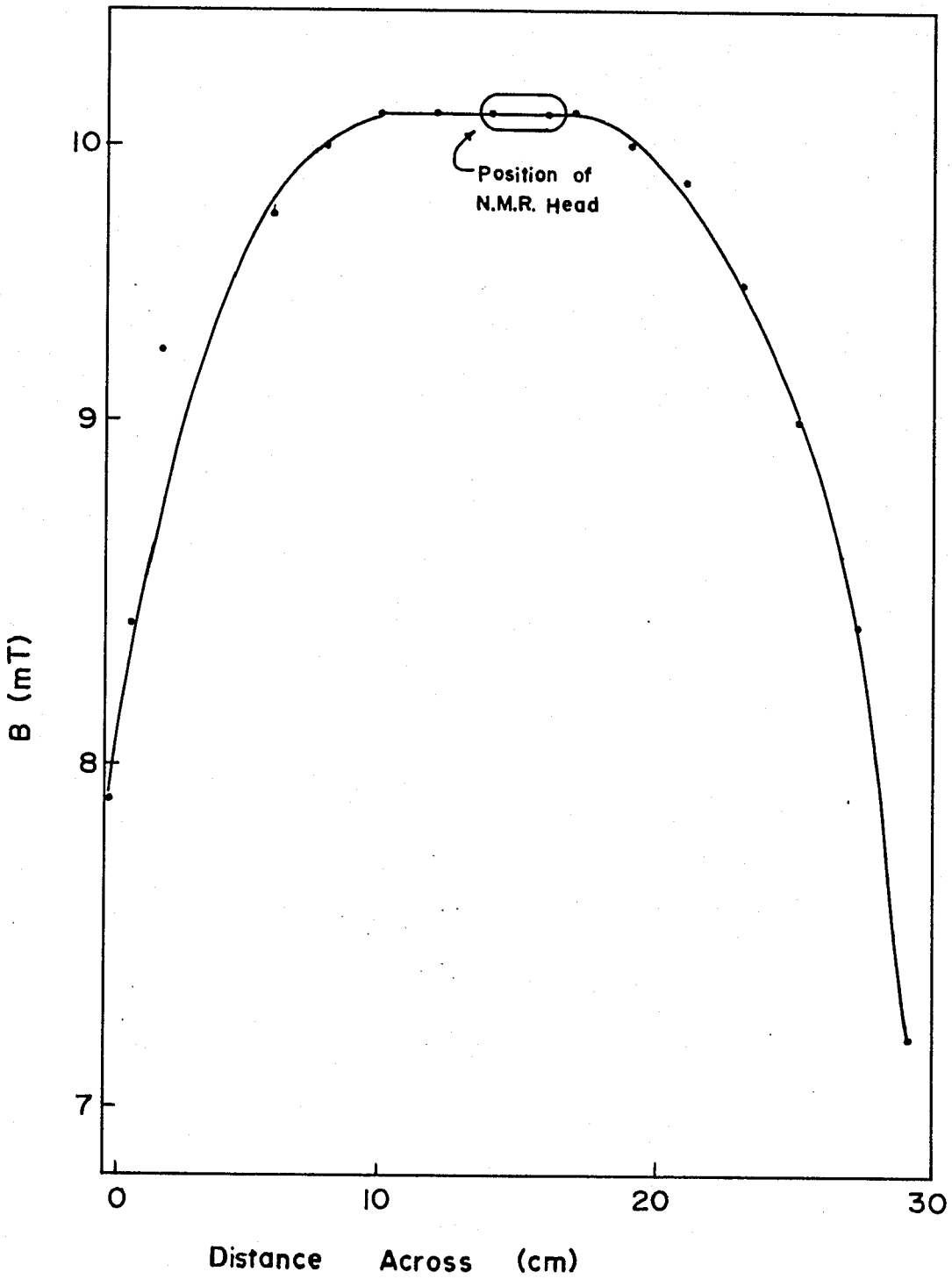

Fig. #16 Field Profile (Horizontal) of Helmholtz Pair

PROCEDURE

INTRODUCTION

A cryostat designed to perform N.M.R. SQUID magnetometer measurements below 1K using magnetic cooling with an indirect helium gas heat exchanger presents several uncommon features which have required the development of a set of experimental procedures. These concern the preparation of the cryostat, the precooling and final cooling stages, the trapping of a stable field B_o for N.M.R., the successive steps in adiabatic demagnetization cooling and the recording of N.M.R. signals. While most of these procedures are well known, it is nevertheless important to summarize them briefly, pointing out important sequences and particular precautions which are essential for a successful run. It is also important to record here as a guide for future users of this cryostat.

(a) Preparation of the Cryostat

After positioning the dewar set in the large Helmholtz pair of coils that will provide the vertical N.M.R. field B_o to be trapped, the cryostat attached to the elevator was carefully lowered into place and the dewar flange sealed. The air inside it was flushed out by circulating helium gas from a compressed gas cylinder for some 8 to 10 minutes. This is advisable for several reasons but in this set-up in particular to ensure that

during cool-down the delicate point contact of the SQUID probe, which is not sealed off, in this instance, is not adversely affected later by freezing water vapour or even by freezing air. Next, the gas heat exchangers operating between the 1K pot and the lower plate were evacuated to primary vacuum. After several minutes it was the 1K pot that was pumped for five minutes to remove any traces of air that could block its intake impedance capillary. Then the valve in the line from the pump to the 1K pot was closed and the pot allowed to fill slowly with helium gas through the intake capillary. The pumps could be stopped at this point.

(b) Precooling to liquid nitrogen temperature

During the evening preceding a run, the liquid nitrogen dewar was first filled and left to evaporate slowly on its own, while the cryostat started cooling. The liquid nitrogen dewar was replenished again later at 3 a.m. by a previously set electric timer and, from then on until the helium was transferred, it was maintained full with an automatic liquid nitrogen level controller. By 10 a.m., the interior had normally reached 80 to 85K. The calorimeter was then pumped to primary vacuum and enough hydrogen exchange gas admitted to bring the pressure to approximately 60 Pa. Evacuation of the calorimeter is done only after the cooling salt is frozen to avoid its dehydration,

in spite of the fact that the salt pill assembly is coated with silicone grease and protected by a plastic sheet envelop. This protection is adequate to slow down the dehydration when exposed to the atmosphere but would not protect the salt if evacuated at room temperature.

Hydrogen plays the role of an efficient exchange gas until it freezes out around 9K. In a calorimeter such as ours, helium exchange gas would be absorbed on the very large cooling area of the salt and its complex insulating supports and structure. The high vacuum pumping speed available to evacuate this exchange gas would be insufficient to remove the helium in a reasonable period of time. This adsorbed helium that would eventually coat all the vital parts with an unsaturated film, thermally connecting the salt and its supports to the 1K pot and possibly the 4K environment. This would preclude the possibility of efficient adiabatic cooling. Hydrogen on the other hand has the disadvantage of freezing out before the interior of the calorimeter has reached 4K. However, around 9K, the heat capacity of the salt and copper is quite small and the normal operation of the exchangers (to be discussed later) is sufficient to cool the interior to 4.2K.

It is interesting to note that if no exchange gas was used at all in the calorimeter, but instead helium was circulated through the heat exchangers to cool the

interior from 77K to 4.2K, it would take four hours after completing the transfer because the cooling capacity of the small amount of gas is so low.

Prior to transferring of liquid helium, the C.R.T.'s were checked and the Helmholtz pair was energized to 12.5 mT after the water to the cooling jacket had been turned on.

(c) Liquid Helium Transfer

Initially liquid helium was deliberately syphoned slowly into the dewar, fully utilizing the high heat capacity of the gas to cool the large mass of the superconducting solenoid. Since the solenoid is located at the bottom of the dewar, the syphon must be long enough to reach the solenoid and effectively cool it with the cold gas. This length makes it quite cumbersome to handle and difficult to position correctly but if proper care is not taken, a great amount of helium could be wasted and still no liquid collected in the dewar. This explains why such a great deal of effort was spent in perfecting a reliable syphon transfer guide.

During the transfer, the 1K pot is continuously pumped to help cool the interior of the calorimeter by drawing in and circulating cool helium gas. With the hydrogen exchange gas, the interior cooled rapidly from 77K almost maintaining an equilibrium with the exterior down to about 9K.

The temperature of the solenoid was monitored by measuring the D.C. resistance of the copper plating on the wire. Another check on the state of cooling of the cryostat was effected by observing the sudden appearance of the triangular pattern of the SQUID electronics on the oscilliscope. This happens as soon as the point contact of the SQUID probes becomes superconducting and occurs before any liquid has collected, since the transition temperature of niobium is 9K.

As soon as the large superconducting solenoid had gone through its transition, the rate of transferring liquid helium was increased. The liquid would then start to collect quite easily. It is easy to find out when the N.M.R. field trap went through its transition trapping the field B_o as then the SQUID would momentarily lose "lock" i.e. the normal, steady triangular pattern on the oscilliscope would rapidly oscillate for three to five seconds.

The cooling of either the 1K pot or the lower stage can be monitored continuously by the corresponding C.R.T. on the null meter of the A.C. bridge and/or the strip chart recorder connected to it.

The level of the liquid helium in the dewar was measured to within $\frac{1}{2}$ cm with a Niomax wire level indicator. Details on the construction and operation of this level indicator is given in the Appendix.

Typically, 18 to 20 liters of liquid helium were needed to fill the dewar if the superconducting solenoid was in place, and 14 liters if it was not.

Helium gas was circulated through the exchangers at a rate of 100 ml per minute to cool the lower stage from 9K to 2.19K (the lamda point). This rate was chosen because it was found that at higher flow rates, the helium gas would not have adequate time to come to thermal equilibrium with the 1K pot and cause the lower stage to warm. At the λ point, the circulation was stopped and the remaining gas was pumped out. Finally, 200 milliliters of gas (at S.T.P.) were readmitted to cool the entire lower stage to 1.3K by superfluid creep. The amount of helium gas present in the exchangers is very critical; too little - and inadequate cooling is observed since thermal isolation is effectively achieved; too much - and heat is conducted down from the 4.2K bath to the 1K pot to the plate which stops the cooling. If the circulation is just stopped after the lamda point is reached and the gas in the exchangers allowed to remain, then the residual volume of liquid and gas is too great and results in no cooling.

(d) Adiabatic Demagnetization Cooling

The field of the superconducting solenoid was turned on and brought up to 2.5T once the pill had cooled to 1.4K. The heat of magnetization of the salt pill was

removed by the helium in the heat exchangers. The temperature of the salt pill was originally monitored by a calibrated Speer resistor attached to the bottom of the pill and fixed there with grease to improve thermal contact.

Prior to demagnetizing, the helium in the heat exchangers was removed by pumping for fifteen minutes.

Various times of demagnetization were tried. Reducing the current by manually turning a rheostat, proved inadequate as the field went from 100 mT to zero too rapidly (less than 20 seconds) causing considerable eddy current heating. A motorized drive was later installed to turn the rheostat at a much slower rate.

(e) N.M.R. Signal

The N.M.R. signals were obtained in a manner similar to that described by Goodchild[13]: a triangular wave from a Hewlett Packard 3310A Function Generator was applied to the VCG IN of a Wavetek model 164 30 MHz Sweep Generator and to the X axis of an X-Y recorder (Hewlett-Packard 7004B). This swept the frequency of the Wavetek about the resonance point and caused the X axis of the recorder to oscillate about its zero. For slow passage conditions, a low driving frequency (approx. 0.01Hz) was used and for adiabatic fast passage, a much higher frequency (approx. 1Hz). The frequency output of the Wavetek was measured with a

General Radio 1192 Frequency Counter. The output of the SQUID electronics was fed into the Y axis of the X-Y recorder to give the N.M.R. tracings (See Figs. 18,19,20 & 23).

For the T_1 measurements of aluminum, the X axis was still driven by the triangular wave but the r.f. function generator was adjusted to operate on the resonance frequency, i.e. causing the maximum N.M.R. signal. After several seconds, the r.f. lead was disconnected and the ensuing output of the SQUID was observed on the Y axis as the disturbed nuclei regained their thermal equilibrium value. To ensure that it was really the decaying N.M.R. signal that was observed and not a change in the base line of the SQUID output, the r.f. cable was disconnected when the frequency was far off resonance and no drift like change in base line was noted.

The SQUID electronics driving the SQUID probe mostly used in this work is a SHE SQUID Control combined with a SHE SQUID System r.f. Head Model 300. This system has three levels of amplification (1, 10 and 100, the latter being used exclusively in the work reported later), four filters on its D.C. output (100, 10, 1 and 0.1 Hz) and a 60 dB, 60 Hz notch filter.

N.M.R. adiabatic fast passage of the proton signal was used to determine the magnitude of the field B_o present in the superconducting niobium field trap[13].

CHAPTER III

COOLING BELOW 1K RESULTS

Due to an essentially untraceable and recurring vacuum microleak in the calorimeter that occurred more often than otherwise, very few leak free runs could be performed but enough that the cooling behaviour of the cryostat could be studied. Thus, in spite of the very adverse conditions, the good runs were sufficient to permit a first evaluation of the cooling capability of the system. The cooling results obtained will be summarized here and commented on from the point of view of doing N.M.R. below 1K in this cryostat.

To obtain the maximum cooling power of the salt, it is important to start from as low a temperature as possible prior to demagnetization[12]. With the helium gas at 10 KPa circulating at a rate of 1.6 ml s^{-1} in the heat exchanger, the temperature of the lower stage to which the salt is thermally tied, was observed to cool from 4K to 2.19K (λ point) in approximately 30 minutes. With the circulation stopped, the temperature decreased further to 1.3K in about 15 minutes. This last portion of cooling is accelerated probably due to the presence of a superfluid HeII film in the heat exchanger tubes between the 1K plate and the lower stage[17]. By magnetizing the cooling salt slowly enough, it was possible, even if the temperature of

the salt rose to 4K and above, to maintain the lower stage below the λ point. A period of $\frac{3}{4}$ to 1 hour elapsed between the end of magnetization and the time necessary to bring the temperature of the salt down close to 1.3K in the presence of the high magnetizing field.

After the salt had cooled to 1.3K, the lower stage was thermally isolated from the 1K pot by pumping out the helium in the heat exchangers. Since the helium was superfluid, this pumping required 15 minutes to reduce the pressure 3 Pa as measured at the top of the cryostat with a Pirani vacuum gauge.

On demagnetizing, the salt cooled quite quickly, following the reduction of the field and reached its lowest temperature of 70mK 10 minutes after the field was brought to zero. During that time the temperature of the plate followed that of the salt cooling further and further as the salt warmed and both proceeded to a common thermal equilibrium. This indicates that there was fairly good thermal contact between the salt and lower stage. The experimental stage reached its lowest temperature of 240mK 15 minutes after the field had been reduced to zero. In the final stage of demagnetizing, the salt showed a sudden warming trend due to eddy current heating in the silver wires and in the copper plate. This heat was eventually absorbed by the salt; however, this heating would adversely affect the

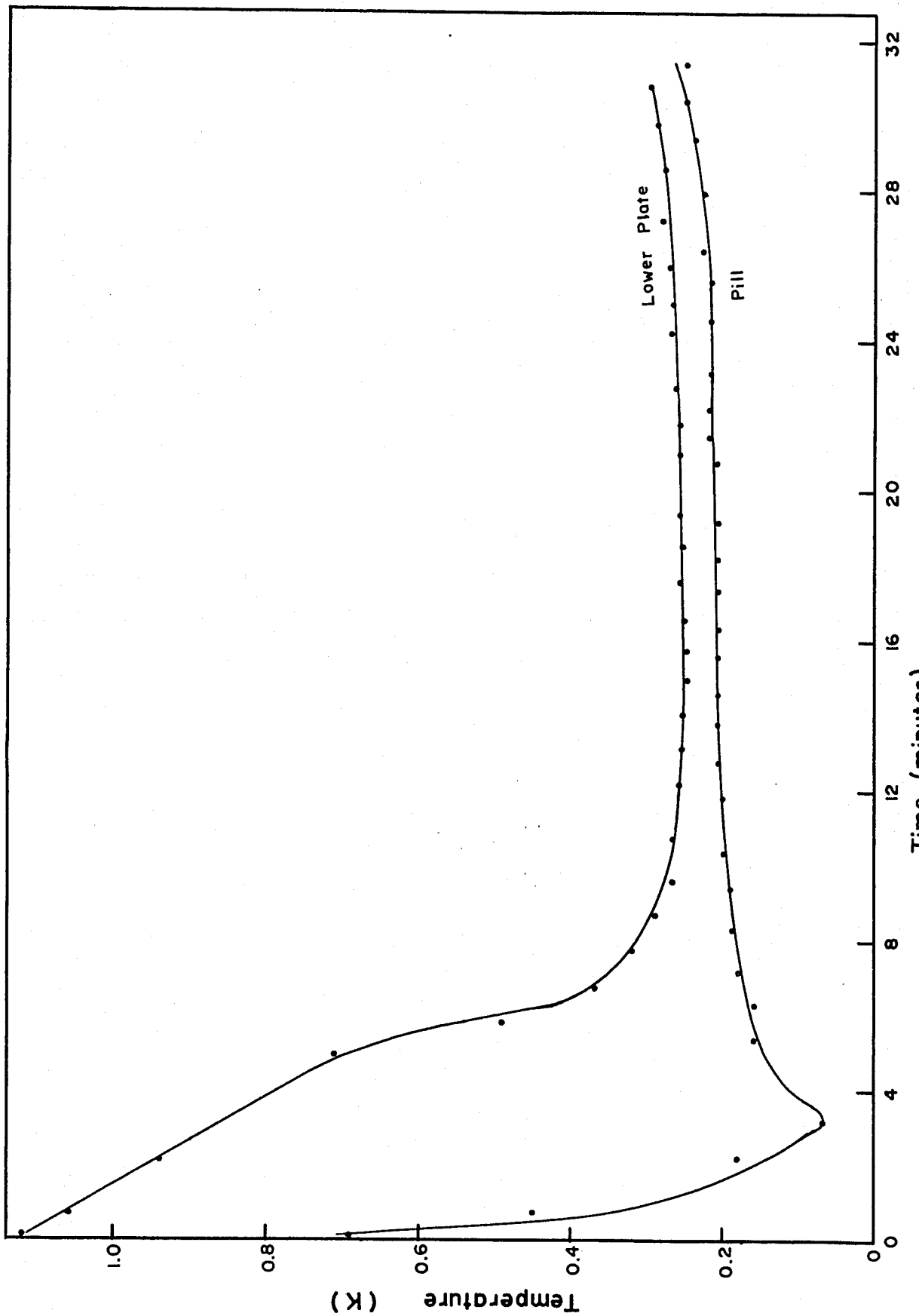

Fig. #17 Temperature versus Time Curve, Lower Stage

lowest attainable temperature.

A calculation showed that as much as 80 μJ of heat would be produced by eddy current heating if the demagnetization was done too quickly, i.e. at a rate greater than 2.3 mT s^{-1} in the last few tens of mT. Slowing the demagnetization rate would still produce excessive eddy current heating because there is a relatively large amount of metal exposed to the fringing field of the magnetizing solenoid. Since there is always a residual heat leak to the lower stage and the salt due to conduction along the supports, vibration and a residual amount of exchange gas, demagnetizing too slowly is not advisable either. Thus a compromise has to be struck to attain the lowest temperature.

The lower stage on which the N.M.R. measurements below 1K must be made, warmed to 1.3K in 45 minutes after reaching its lowest temperature. The heat leak mentioned above was estimated to be between 9 and 10 μW (90 to 100 ergs-s^{-1}). To evaluate the heat leak, one must take into account the total masses of copper and silver and the mass of the cooling salt, and calculate from their known heat capacities the amount of heat necessary to warm them between two values of temperature in the observed time interval separating them.

i.e.

$$\dot{Q} = \frac{1}{t}\int (n_s Cp_s + n_{Cu} Cp_{Cu} + n_{Ag} Cp_{Ag})\, dT \qquad (36)$$

Here the exact amount of copper involved was not known accurately enough to do a precise calculation.

It was observed that the lower stage warmed from 240mK to 300mK in about 22 minutes. This would appear sufficient to perform several adiabatic fast passage N.M.R. measurements and allow several measurements of T_1. Finally it is a sufficiently long period of time to do a slow passage recording of a N.M.R. signal around 300mK.

It is assumed here in all cases that the sample to be investigated is a metal that has a relaxation time T_1 not exceeding several tens of seconds. (eg. $T_1 \approx 6s$ for ^{27}Al at 300mK)

During the good runs, the pressure of the high vacuum line leading into the experimental chamber was in the vicinity of 100 μPa as read on a cold cathode discharge gauge at the top of the cryostat and hence at room temperature. The pressure in the calorimeter containing the salt is probably lower by at least a factor of ten. Indeed the pressure may have been even lower, possibly between 10 μPa and 10 pPa because the cold salt and the graphite have a fairly large cryopumping effect.

CHAPTER IV

ALUMINUM RESULTS

INTRODUCTION

This section deals with the advantages and some preliminary results on the use of the ^{27}Al N.M.R. signal for the purpose of thermometry. The magnetic properties of the metal to be used for the thermometer are very important since it often happens that even minute quantities of magnetic impurities of electronic origin add unwanted and poorly known temperature dependent contributions to the overall magnetization. Moberly et al (to be published) found that iron and manganese impurities in aluminum do not contribute to the magnetization down to 10 mK. Thus aluminum is likely to be a reliable substance for N.M.R. thermometry even if it is not in the purest state. Another interesting feature is that the nuclear spin-lattice relaxation time of aluminum is one of the longest, with a Korringa constant of 1.8 s-K.

The N.M.R. signal was studied at three different temperatures, 4.2K, 3.4K and 1.35K, as a function of B_1 and in a constant field B_o (13 mT) for two different forms and origin of samples: aluminum foil and powder.

To get meaningful readings, a thermometer must

be in thermal equilibrium with the bath whose temperature it is measuring and it is important to avoid any thermal gradients in the thermometer itself. A metal foil is likely to fulfil these conditions rather well as a continuous strip should show good heat conduction even at low temperatures and maintaining the entire sample reasonably well at the same temperature.

The actual sample studied was a strip of Alcan Aluminum Foil, 200 mm long by 15 mm wide by 26 μm thick with a mass of 210 mg (or approx. 4.7×10^{21} nuclei). A strip of mylar sheet of the same width but 30 mm longer was laid on top of the foil and glued to one end. The two sheets were rolled together into a tight coil. The separation by the mylar was to prevent electrical contact between the layers and allow the r.f. to fully irradiate the sample. A single small strip of mylar was wrapped end for end on the sample and an r.f. coil consisting of 15 turns of #40 AWG copper wire was wound on. The sample was then inserted into the N.M.R. head and cast into place with Araldite to improve the thermal contact to the head and lower stage[14]. With these precautions, it was hoped that the temperature of the foil would be the same as that measured with a C.R.T. attached to the lower stage.

As the results with the foil were not satisfactory (to be discussed later), it was decided to investigate aluminum powder. The powder was made by filing an aluminum rod (4N purity) and passing the powder through a 100 mesh sieve. As viewed with a microscope; the grains of powder appeared as rectangularly shaped turnings rolled into a sphere with an average radius of 40 μm. A sample of approximately 90 mg (2×10^{21} nuclei) was thus prepared. The powder was packed into a teflon tube (4.8 mm I.D.), permeated with molten parafin wax and allowed to cool. The solidified sample was later removed and an r.f. coil wound on it as for the foil sample. It was then inserted into the N.M.R. head and sealed with Araldite.

The reason for using an r.f. coil directly wound on the sample rather than a saddle shaped type of r.f. coil pair as other investigators have done, is to minimize the flux reduction factor due to the geometrical arrangement of the magnetometer. Following the analysis developed by Goodchild[13], let us define by $\Delta\Phi_c$ the flux change detected by the flux transformer coil and by $\Delta\Phi_s$ the flux change occurring in the sample undergoing resonance. Let A_s be the cross sectional area of the sample, A_c be that enclosed by the flux transformer coil and A_t, that

enclosed by the Nb field trap. Goodchild has defined as a "reduction factor" the ratio

$$\frac{\Delta\Phi_c}{\Delta\Phi_s} = \frac{A_T - A_C}{A_T - A_S} \qquad (37)$$

It expresses the ratio of the flux change recorded by the magnetometer with respect to the flux change actually taking place in the sample. It is a sort of "filling factor" which would have a value approaching 100% in the case of a transformer coil tightly wound on the sample (i.e. when $A_c = A_s$).

For aluminum, A_c, expressed in percentages of the field trap area is 44.4%, A_s is 25.2%. Therefore $\Delta\Phi_c/\Delta\Phi_s$ is 0.74. Thus 26% of the signal is lost. The method of calculating flux loss is only approximate as it assumes that the flux distribution is a step function. Merely by increasing the area of the trap by a factor of two, the signal can be increased by 20% so that $\Delta\Phi_c/\Delta\Phi_s$ would become 0.89.

EXPERIMENTAL RESULTS

A typical ^{27}Al signal with the aluminum foil sample at 1.35K is shown in Fig. #18 with the peak at a frequency of 151 KHz corresponding to 13.6 mT in agreement with the field determined by the frequency of a proton signal also observed and originating from the mylar. The signal with the powder sample is shown in Fig. #19. The centre frequency is at 142 KHz

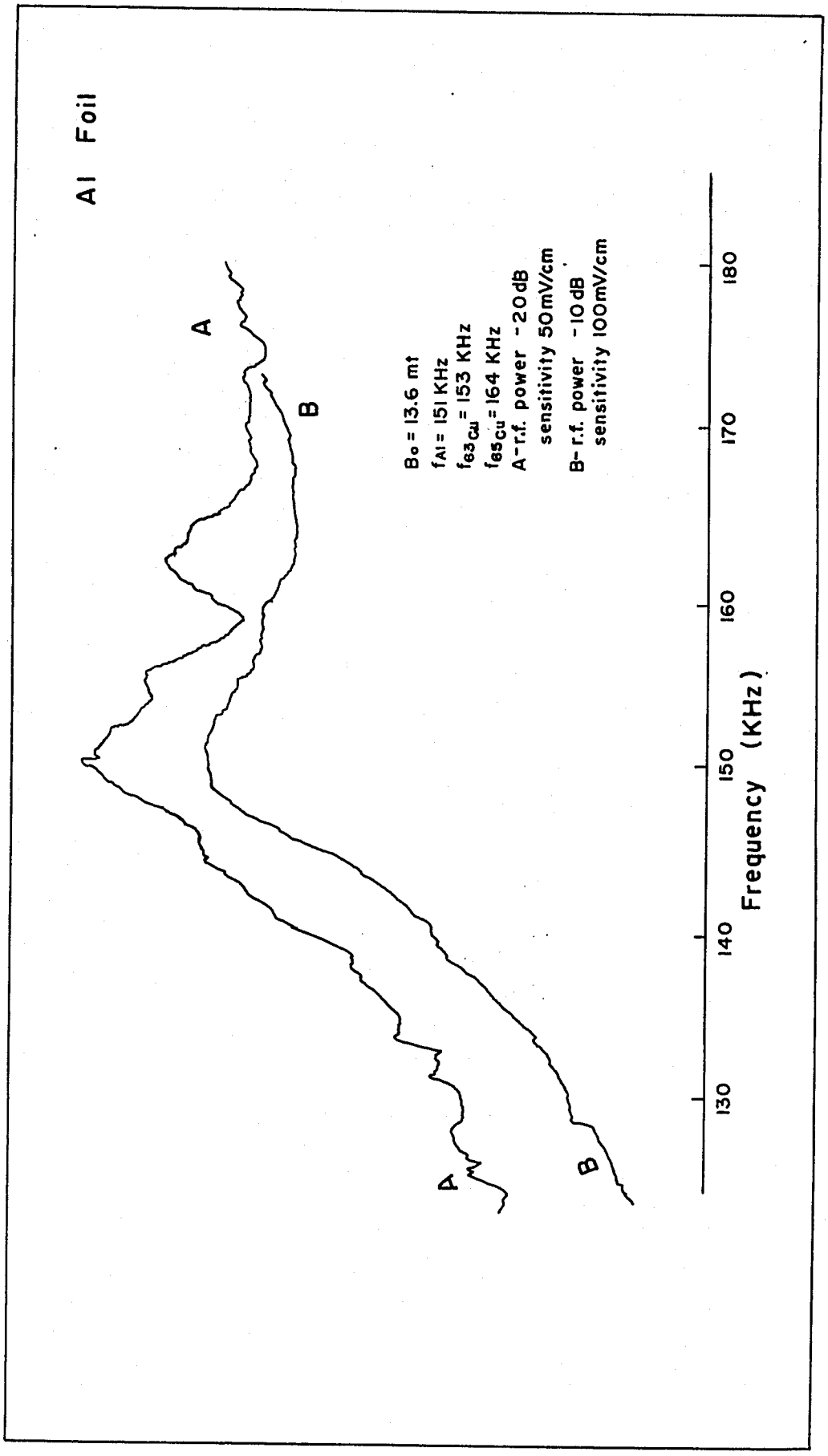

Fig. #18 Typical N.M.R. Tracing, Al Foil

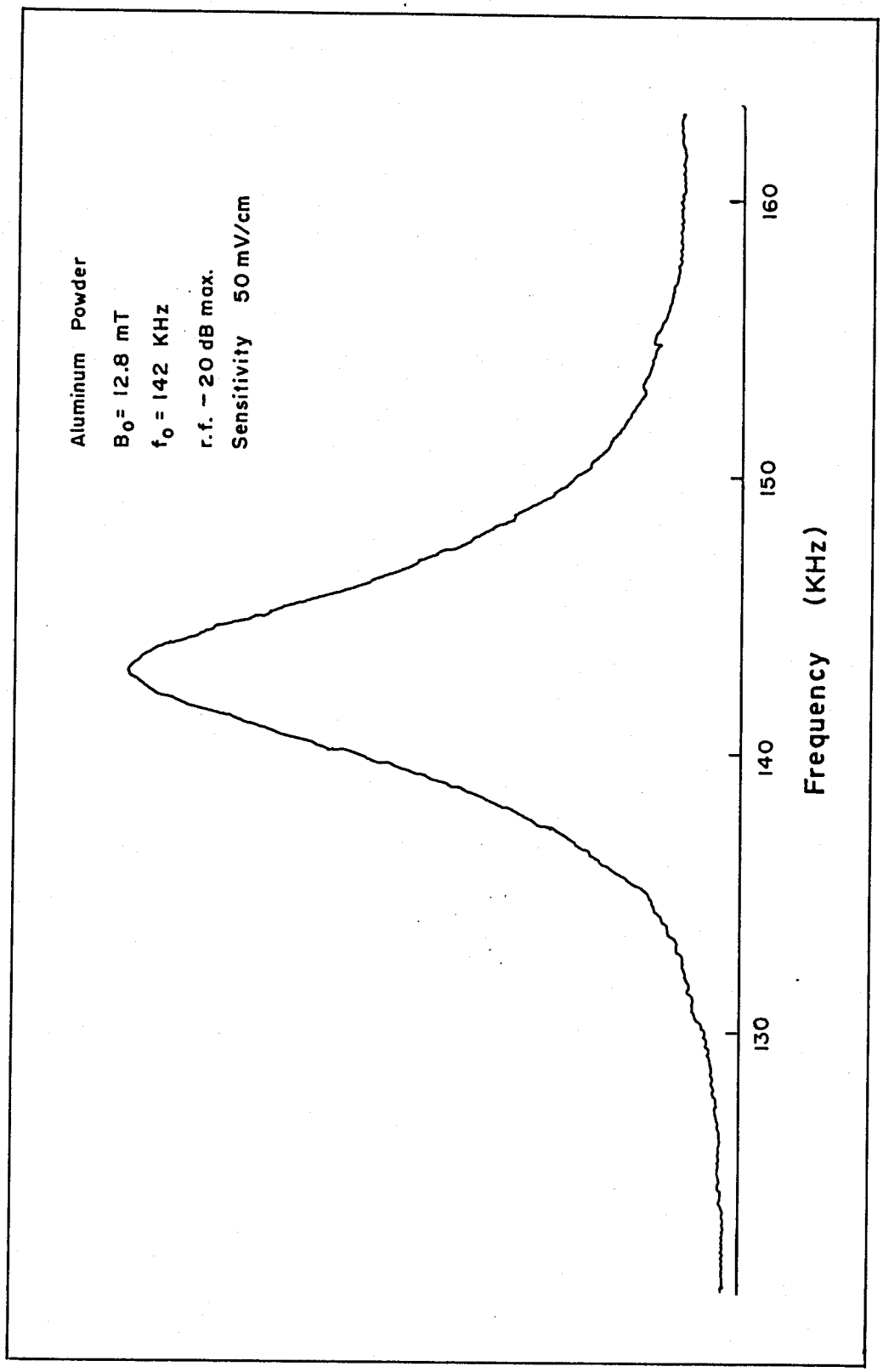

Fig. #19 Typical N.M.R. Tracing, Al Powder

corresponding to a field of 12.8 mT. The frequency markers were introduced manually on the tracing by the experimenter reading it off the frequency meter and are accurate to better than 0.1%. The tracings were obtained as the frequency was swept up and down past the resonance at rates approaching slow passage conditions. The values of B_o used in the studies of the foil sample were 25.0, 13.6 and 12.8 mT and for the powder, 13.6 and 14.2 mT. The signal to noise ratio was 63:1 with a 1 Hz filter in the SQUID control electronics for the powder at 4.2K, 10:1 with no filter for the foil at 1.35K with B_1 equal to 16 μT and 30:1 for B_1 equal to 51 μT.

Measurements of the line widths at half intensity gave 0.95 $\pm$ 0.03 mT for the foil and 0.71 $\pm$ 0.02 mT for the powder in fields of 12.8 mT and 13.6 mT respectively. The large drift in the base line made line width remasurements of the foil impossible to do accurately.

The relaxation rate of aluminum powder at 4.2K was studied and a typical tracing is shown on Fig. #20. The average of a number of such readings for T_1 is 0.37 $\pm$ 0.04 seconds.

To determine the field factor of B_1, it was found experimentally that for low power, B_1 is

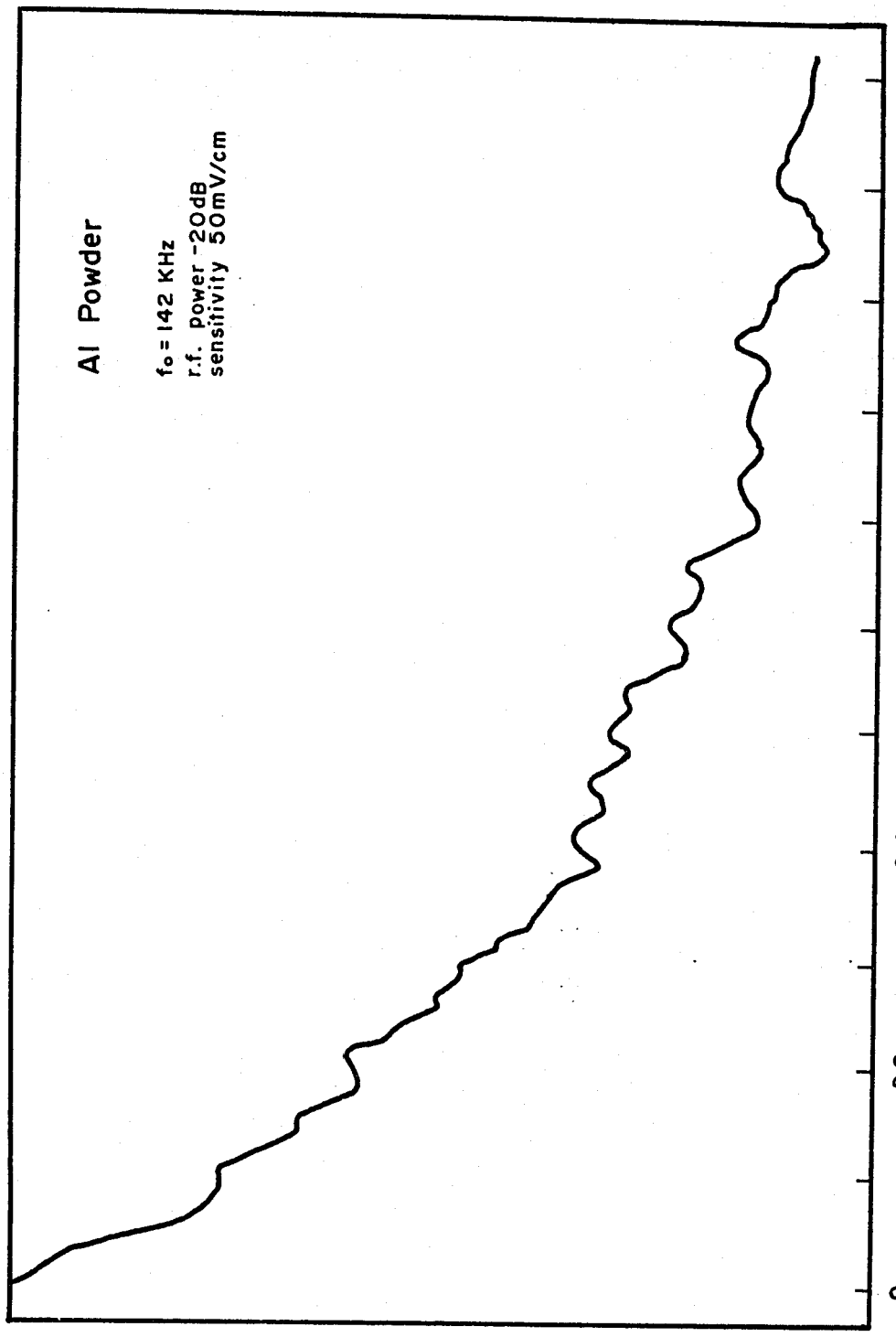

Fig. #20 Relaxation Time, Al Powder

proportional to the voltage output of the Wavetek. Equation 18 can be rewritten as

$$S.H. = \frac{a \cdot V^2}{1 + bV^2} \qquad (38)$$

A graph of signal height versus voltage is plotted for the aluminum signal and shown in Fig. #21 and a least squares fit was done using equation 37 to find the voltage corresponding to half of the saturation signal. Then from equation 19 a calculation gives a field factor of $110\mu TV^{-1}$. The fit to the data is good but it must be noted that the theoretical line only approximates the experimental points. The values of the constants were found to be 11.77 for a and 0.4805 for b, but with an error of 10%. The profile of the field of the r.f. coil was then mapped (See Fig. #22) and it is immediately apparent that B_1 is not uniform throughout the sample, varying by as much as a factor of three. This could explain the variation in the theoretical line from the experimental points.

DISCUSSION

The measured line widths of aluminum are tabulated below and compared to previous results

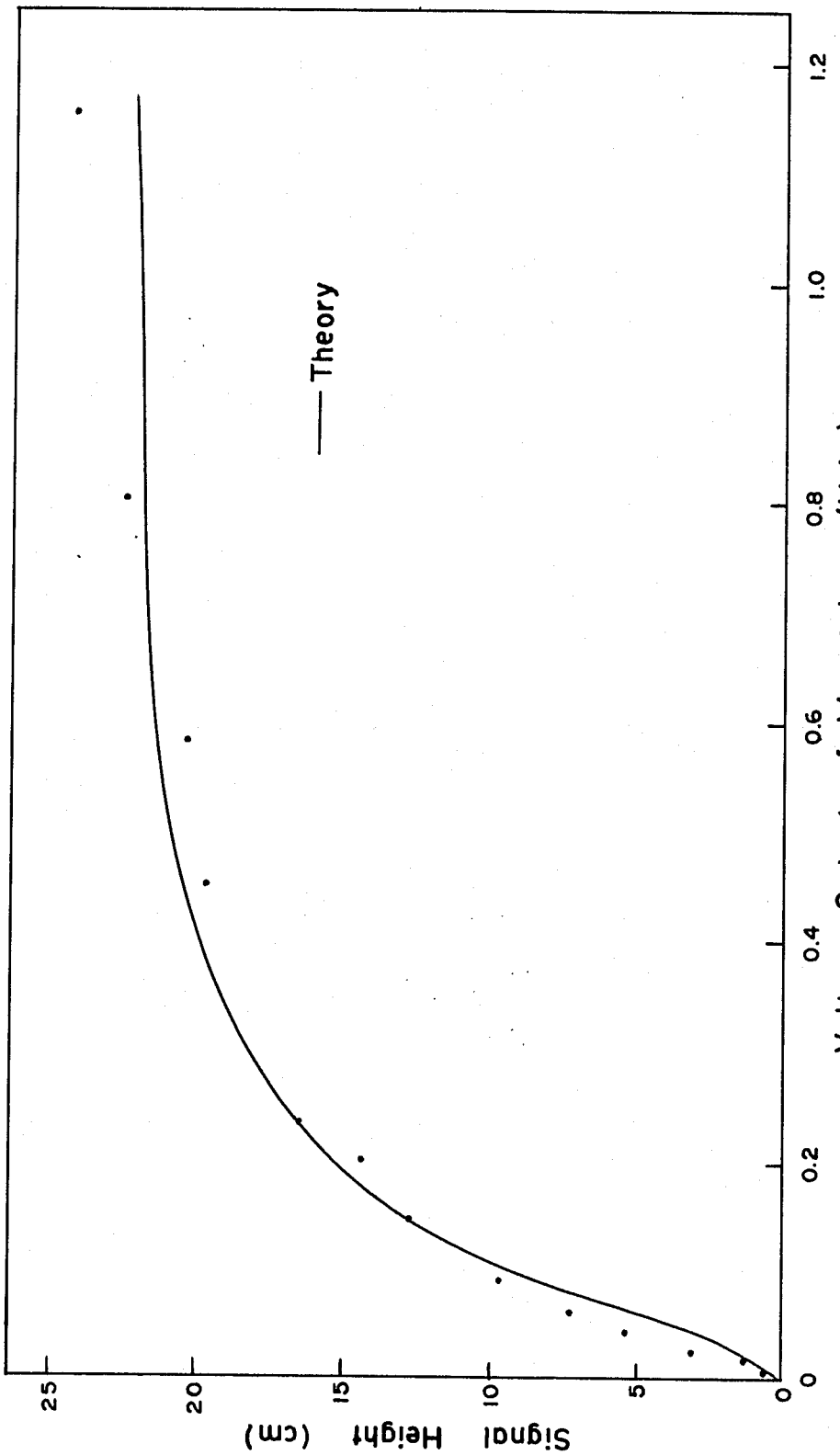

Fig. #21 Graph of Saturation versus r.f. Amplitude, Al Powder

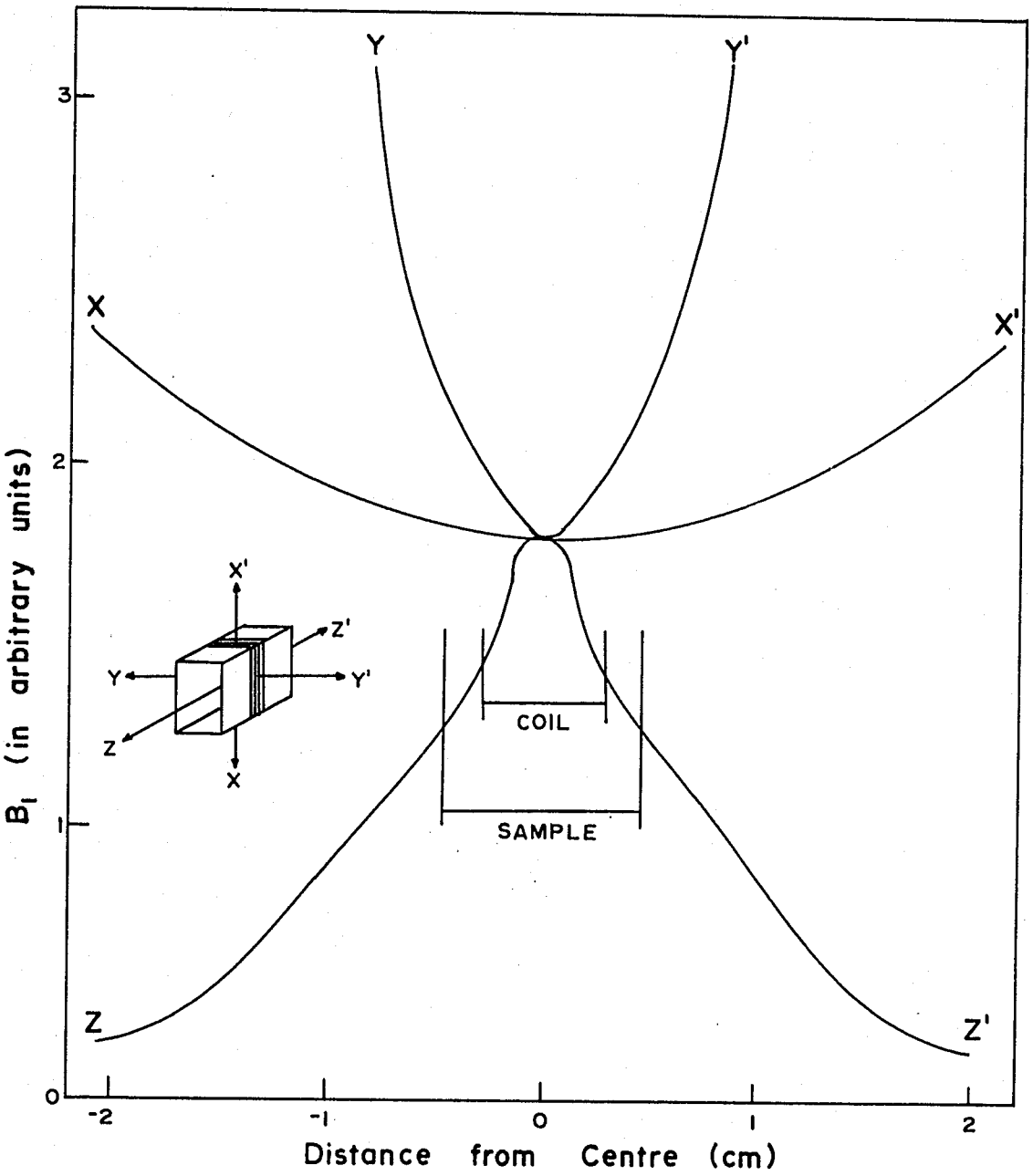

Fig. #22 Field Profile, r.f. Coil

0.71 ± 0.02 mT	present results powder
0.95 ± 0.03 mT	present results foil
0.88 mT	Seymour[24]
0.81 mT	Poulis[25]
0.84 mT	Knight[26]

The difference in line widths between the foil and the powder is probably not due to a deformation in the lattice structure of the foil from the rolling process in manufacture which would cause a broadening in the line width[27]. The lattice parameters of the foil and powder were measured using X-ray powder patterns and analysed[28] giving values of 404.6 pm for the powder and 404.5 pm for the foil. It would appear that the crystal structure is identical for both of them and yet a chemical analysis[29] has shown that there is 1% iron in the foil that is not in solution. Symko[3] notes that iron as a trace impurity has no contribution to the bulk magnetism and hence no effect on line widths or relaxation time, but does not comment for a large amount of iron dispersed through the foil. It is not known how iron is arranged in the foil, X-ray analysis has failed to reveal whether the iron is there as an impurity crystallite scattered randomly through the metal or on the surface left there by the rolling process in

manufacturing.

The difference in the line widths then may be attributed to the high concentration of iron which does form some kind of local moment.

The values of Seymour, Poulis and Knight were calculated from the position of the maximum and minimum in the derivative of the absorption curve, whereas the values for the powder are measured for the line width at half intensity which may not be an equivalent method.

The results for the relaxation time of aluminum, 0.37 ± 0.04s is in good agreement with the published data[3, 30]. Most of the error in T_1 is caused by the noise in the relaxation signal and not in base line drift. This noise is a difficult problem since it can not be removed by placing filters in the output of the electronics.

CHAPTER V

LITHIUM NIOBATE RESULTS

Introduction

Due to the enhancement of the N.M.R. signal with decreasing temperature, it was decided to try to observe the ^{7}Li signal and the evasive ^{93}Nb signal below 4.2K.

Both ^{7}Li and ^{93}Nb have an electric quadrupole moment. The lithium N.M.R. spectrum is easily observed and as its quadrupole coupling coupling constant e^2qQ/h, is small, it is only weakly affected by impurities and temperature, whereas Peterson et al[6] have shown how elusive the ^{93}Nb lines are in lithium niobate. This is easily explained on the basis of the large quadrupole coupling constant of 22.02 MHz and on the basis of the difficulty of obtaining the niobate samples in exact stoichiometry because slight imperfections widen the lines and make their observation very difficult.[6,7&9]

All measurements were done on a single crystal donated to us by Dr. Feigelson of Stanford University. The original crystal, as supplied, was comprised of the seed crystal and the top of the pull and was reputedly

exactly stoichiometric. The seed crystal was cut from the bulk of the sample with a wire saw and has the following dimensions; 3 mm wide, 3 mm thick and 11.4 mm in length with the "c" axis of the crystal parallel to its length.

The sample had 24 turns of #40 AWG copper wire for the r.f. coil that completely encompassed the crystal. The measured inductance of the r.f. coil at 7.9 MHz is between 5 and 7μH. The crystal was then glued to the delrin sample holder and inserted into the head of the N.M.R. magnetometer. Since the sample holder fits the bore of the N.M.R. head quite snugly, this allows accurate positioning of the sample whose alignment to B_o, the trapped field, should be within 3°.

Due to the small area of the sample (9 mm^2 or 9.9% of the total area enclosed by the field trap), the filling factor will be quite low i.e. 0.61 or 39% of the signal is lost. This is to be compared with the aluminum which had only a 26% loss.

Results

Due to the persistent leak in the calorimeter, the N.M.R. magnetometer could not be cooled and all measurements were done at 4.2K. A typical recording of the ^7Li signal in slow passage mode is on page 84 Again the tracings were done by increasing and decreasing

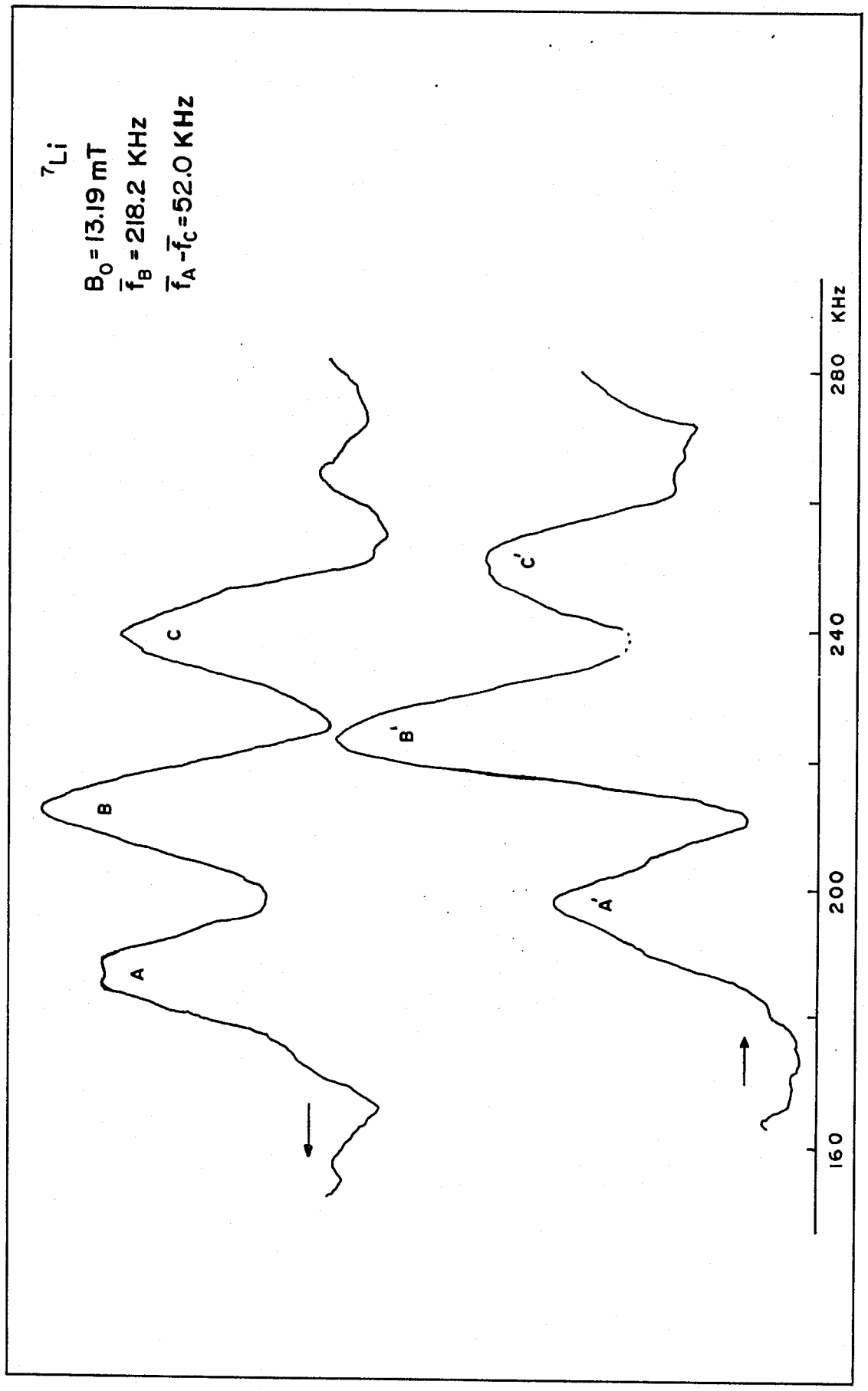

Fig. #23 Typical N.M.R. Tracing, $LiNbO_3$

the frequency to sweep through resonance. The centre line frequency of the $\pm \frac{1}{2} \rightarrow \mp \frac{1}{2}$ transition is at 218.3 ± 0.2 KHz corresponding to 13.19 ± 0.02 mT which agrees with the field obtained from the proton signal. The signal to noise ratio is 30:1 for a 1 Hz filter at the output of the SQUID electronics. The filter introduces a delay in the signal being fed into the X-Y recorder. Therefore, when the sweep is done by increasing the frequency, the position of the three peaks will be shifted to the right, and for decreasing the frequency, the peaks will be shifted to the left. The true centre frequency of the peaks will be obtained by averaging the peak positions. The frequency markers were done manually on the tracing and have an accuracy of 0.1%.

The separation between the peaks of the satellites directly gives the coupling constant for ^{7}Li in $LiNbO_3$ where θ, in equation (27), the angle between B_o and the "c" axis, is zero as is the case here. An average of several readings gives 52 ± 1 KHz.

The line intensities in the N.M.R. spectrum in the case I = 3/2, must be related as 3:4:3[31]. However the presence in the crystal of various defects such as impurities, vacancies and dislocations leads to a decrease in the intensity of the individual lines,

the decrease occurring in the intensity of the satellites first. Thus the intensity of the satellites is a measure of the degree of crystal perfection[8].

The intensity of the three peaks was measured by summing the heights of the corresponding peaks for the two sweeps of increasing and decreasing frequency as the scan was not a true slow passage mode. This would allow for any relaxation effects which were quite long, in the order of 9 seconds or longer[32]. The measured ratios of the intensities are 2.7:4:2.7 or about 0.9 of the theoretical value of the intensities for the satellites.

The technique of Jach[33] was attempted in an effort to observe the low field N.M.R. spectrum to obtain information on the quadrupole spectrum of ^{93}Nb. The spectrum should have peaks at 1, 2, 3 and 4 MHz. Unfortunately there was some coupling of the r.f. to the SQUID which caused the electronics of the SQUID to "unlock" above 1 MHz and thus no signal could be detected.

Discussion

The value of the coupling constant in this work is compared to previous results

Author	e^2qQ/h (KHz)	Comments
Burns (1962)	46	independent of T
Peterson et al (1967)	55.2 ± 0.4	room temperature
Bogdanov et al (1968)	53	room temperature
Lamarche (1976)	51 ± 1	4.2K
This work	52 ± 1	4.2K

The value of $\Delta\nu$ is in agreement with the previous results of Bogdanov and Lamarche, but is higher than Burns and lower than Peterson. The measurements of Burns were done on a powder which makes interpretation of results extremely difficult. Peterson et al[6] have done extensive measurements of $\Delta\nu$, the distance between satellite peaks as a function of θ, which is given by equation (21). Assuming that the coupling constant of Peterson is valid at 4.2K, then the error in alignment of the "c" axis to the applied field B_o is 11°. This error is improbable as the "c" axis is along the length of the sample and the alignment could not be worse than 3° which would only change $\Delta\nu$ by less than 1 KHz.

This difference may be significant and may be explained in terms of a temperature dependence despite the findings of Burns[5], or the sample may have been slightly imperfect[32]. In this set of experiments, the relaxation rate, T_1, was not measured which is a good

indicator of the presence of crystal defects. However, judging by the intensity of the satellite lines, the number of defects are indeed few.

CHAPTER VI

CONCLUSIONS

The high sensitivity and rapid response of the SQUID magnetometer makes it an extremely useful instrument to detect N.M.R. phenomena in low temperature experiments. The preliminary results reported in this thesis show that the N.M.R. signal of aluminum is a promising material for thermometry below 4.2K.

The measured line widths of ^{27}Al are 0.71 $\pm$ 0.02 mT for a powder of pure metal and 0.95 $\pm$ 0.03 mT for a commercially available foil in fields of 12.8 mT and 25.0 mT respectively. A relaxation time of 0.37 $\pm$ 0.04 s at 4.2K was obtained for the powder in a field of 12.8 mT. The temperature dependence of the signal amplitude of the aluminum foil was found to be close to what can be predicted from the Bloch equations.

The difference in line widths between the foil and the powder is probably attributable to the presence of iron in the foil. Further studies should be done to observe if the high concentration of iron causes departure from Korringa's relation.

The N.M.R. spectrum of ^{7}Li was observed in $LiNbO_3$ and the value of the coupling constant e^2qQ/h,

was measured to be 52 ± 1 KHz. The presence of crystal defects and impurities is not apparent, considering that the observed results for the relative intensities of the satellite peaks and main peak is indeed very close to that predicted by theory.

N.M.R. thermometry can be improved by choosing another substance whose nuclear spin system has a shorter spin-lattice relaxation time and hence will return to thermal equilibrium much quicker at lower temperatures after a measurement has been completed. Less time will be needed to measure this shorter T_1 and thus it will not be as adversely affected by base line drift. This short relaxation time does, however, require a recording instrument that can trace a very fast signal. The best candidate for low temperature thermometry is metallic tin whose Korringa constant is 0.03 K-s.[3] This system also has the advantage that magnetic impurities do not form local moments that would affect the relaxation rate.[3] However with its extremely short relaxation time at high temperatures, the SQUID magnetometer may not be capable of following the fast change in magnetization from the decaying signal. A study would have to be done to determine the shortest T_1 that the SQUID can accurately follow.

At such low temperatures, it would be advantageous to use a finer powder for the sample than the 80μm diameter used in our experiments to reduce the eddy current heating, even though it is quite low.

With the development of the recurring microleak continuously admitting helium gas into the calorimeter, it was not possible to cool the N.M.R. head much below 4.2K. During the first experiments to determine the cooling capability of the cryostat, the lower stage did cool to 240 mK but the N.M.R. head was not yet mounted. After the N.M.R. head was attached, the experimental plate was cooled only by the 1K pot to 1.35K. It was then that the microleak developed and all means of leak detecting failed to discover the source of the leak. Due to this untraceable leak and in an effort to reach even lower temperatures than 240 mK, the cryostat will have to be completely rebuilt and it can incorporate other improvements as well.

In the present apparatus, with virtually all of the lower volume in the dewar occupied by the calorimeter and the large superconducting solenoid with its supports and persistent mode switch, there is no space to mount a small solenoid to supply the field B_o for the

N.M.R. field trap. This necessitated the use of the large Helmholtz pair that, although the field from them was extremely uniform, the maximum available field was only 15 mT. This field is much below the critical field of 54 mT necessary to destroy the superconductivity in the aluminum powder.

To make room for a second solenoid that will fit inside the supports of the large superconducting solenoid, the lower stage will have to be greatly reduced in size. This can be done by using the r.f. shield of the N.M.R. head as a direct thermal link between a small heat exchanger located at the top of the shield and the salt pill situated below (See Fig. #24 and 25). This will reduce the overall diameter of the experimental stage to less than 25 mm. This will also decrease the amount of copper that has to be cooled to a fifth of its original mass and hence a lower temperature should be reached after demagnetizing the salt.

The lower heat exchanger will be a larger modified version of the one previously described in section 6 of Chapter II. There will be a deeper cut into the plug to increase the contact area for the exchange gas (See insert in Fig. #25).

We would recommend abandoning the single r.f. coil wound directly on to the sample and have instead,

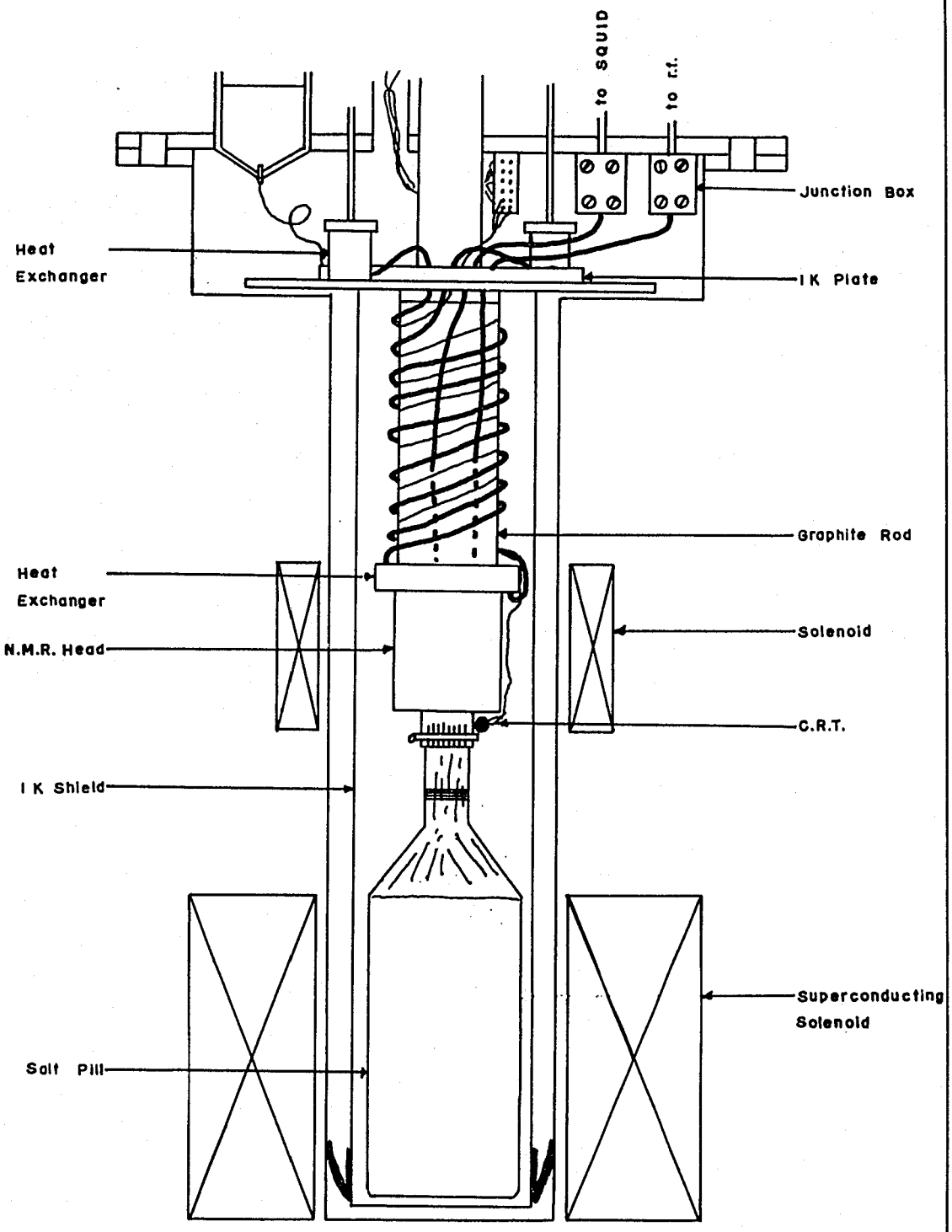

Fig. #24 Proposed Calorimeter

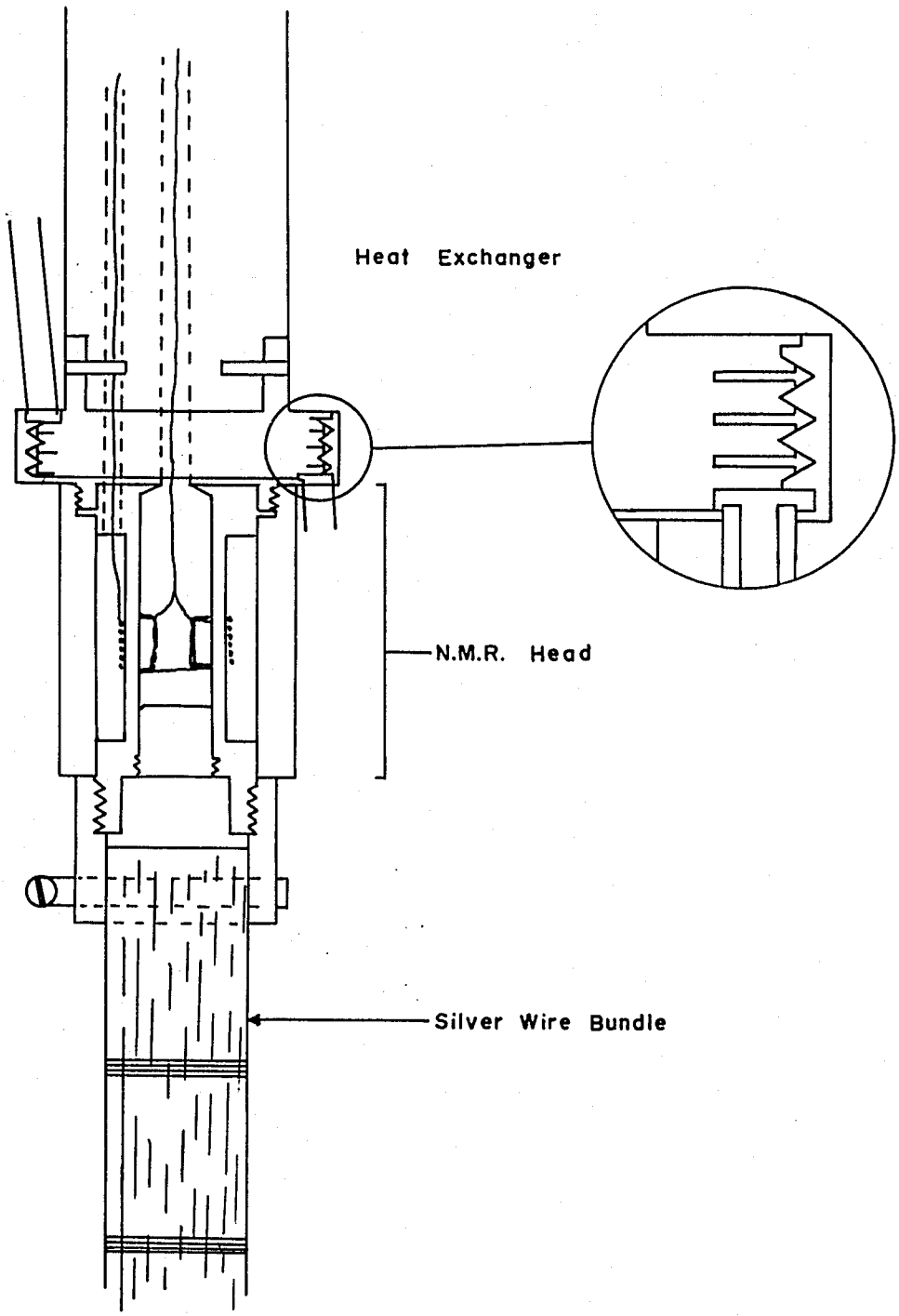

Fig. #25 Details of Proposed Lower Stage

a permanently mounted pair of saddle coils. Access to the sample area in the shield will be by a small plug that screws in from the bottom. The salt pill will be attached to a threaded section on the r.f. head by a slotted copper collar. The r.f. head and the salt pill will be supported by the niobium field trap that will screw onto the heat exchanger.

The entire lower stage will be supported by a single, solid graphite rod 15 mm in diameter and 100 mm long. The heat leak down the graphite should be quite small, less than 100 nW (1 erg-s-1).

By using the r.f. shield as a support, the overall length of the cryostat will be increased by 45 mm. To help in keeping the tail as short as possible, a coil of copper refrigerator tubing (2.4 mm O.D.) soldered to a thin copper plate will be used as the continuously operating refrigerator instead of the present 1K pot. The impedance capillary intake from the 4K bath to the 1K plate will remain the same. Mounted on the plate will be two similar heat exchangers in the inlet and outlet lines of the lower stage. These will be of the design previously described in section 6 of Chapter II; but modified to fit the geometry. Instead of the helium entering at the top and leaving at the bottom, it would enter at the top and leave at the side (See Fig. #24).

The capillary lines to the lower stage will be made of cupro-nickel and have dimensions of 2 mm O.D., 1 mm I.D. and 400 mm long. The expected heat leak down both will be slightly greater than 400 nW.

All capillaries and electrical leads will pass through an opening between the coils near the center of the 1K plate to thermally anchor them at 1K and allow an easy passage to the experimental area.

To reduce eddy current heating, the r.f. leads and saddle coils will be made of niobium wire. The capillary shielding the leads will be superconducting lead instead of cupro-nickel or stainless steel to decrease heat flow down the shield from the 1K plate. Both the r.f. and pick-up coil will be connected to the exterior of the calorimeter through two separate junction boxes (See Ch. II, sec.8) encased in sheets of superconducting lead.

The leads to a C.R.T. mounted in the experimental stage will have to be made of a non-superconducting metal. It was found that the lead plated manganin wires trapped a field and when they vibrated, this produced a low frequency magnetic field which was picked up by the r.f. leads and fed into the pick-up coil in the N.M.R. head and then to the SQUID.

Finally the salt pill, N.M.R. head and lower heat exchanger would be completely wrapped in several

layers of aluminized ½ mil mylar to reduce heating by radiation.

It is expected that since the heat leak will be quite low, around 600 nW, and the mass of the experimental stage will be small, the N.M.R. head can be cooled much below 100 mK, allowing lower temperatures to be reached and longer times to conduct a more thorough investigation of N.M.R. thermometry.

BIBLIOGRAPHY

1. R.E. Walstedt, E.L. Hahn, C. Froidevaux and E. Geissler, Proc. R. Soc., A284, 499 (1965).
2. M.I. Aalto, H.K. Collan, R.G. Gylling and K.O. Nores, Rev. Sci. Inst., 44, 1075 (1973).
3. L.A. Moberly and O.G. Symko, IEEE Transaction Magnetics, Vol. MAG-13, 358 (1977).
4. O.G. Symko, Temperature - Its Measurement and Control in Science and Industry, 4, Part 2, 1239 (1972).
5. G. Burns, Phys. Rev., 127, 1193 (1962).
6. G.E. Peterson, P.M. Bridenbaugh and P. Green, J. Chem. Phys., 46, 4009 (1967).
7. G.E. Peterson, P.M. Bridenbaugh, J. Chem., Phys., 48, 3102 (1967).
8. V.L. Bogdanov, V.V. Lemanov, V.P. Klyuev and S.A. Fedulov, Soviet Physics, Solid State, 10, 886 (1968).
9. G.E. Peterson and J.R. Carruthers, J. Solid State Chem., 1, 98 (1969).
10. E. Schempp, G.E. Peterson and J.R. Carruthers, J. Chem. Phys., 53, 306 (1970).

11. G.E. Peterson and A. Carnevale, J. Chem. Phys., 56, 4848 (1972).

12. O.V. Lounasmaa, Experimental Principles and Methods Below 1K, Academic Press Inc., London (1974).

13. R.G. Goodchild, Unpublished Thesis (1975).

14. D.J. Meredith, G.R. Pickett and O.G. Symko, J. Low Temp. Phys., 13, 607 (1973).

15. A.C. Chapman, P. Rhodes and E.F.W. Seymour, Proc. Phys. Soc., 70, 345 (1956).

16. C. Kittel, Introduction to Solid State Physics, 4th Edition, John Wiley and Sons, Inc., (1971).

17. J.R.G. Keystone, A. Lacaze and D. Thoulouze, Cryogenics, 8, 295 (1968).

18. L.E. DeLong, O.G. Symko and J.C. Wheatley, Rev. Sci. Inst., 42, 147 (1971).

19. A.W. Johnson, Unpublished Thesis.

20. M.C. Hetzler and D. Walton, Rev. Sci. Inst., 39, 1656 (1968).

21. D. Halliday and R. Resnick, Physics Parts I and II, John Wiley and Sons, Inc., 810 (1967).

22. E.P. Day, Phys. Rev. Lett., 29, 540 (1972).

23. A. Roth, Vacuum Technology, North-Holland Pub. (1976).

24. E.F.W. Seymour, Proc. Phys. Soc. A, 66, 85 (1953).

25. N.J. Poulis, Physica, 16, 373 (1950).

26. W.D. Knight, Phys. Rev., 76, 1259 (1949).

27. A. Abragam, The Principles of Nuclear Magnetism, Oxford (1961).

28. N.F.M. Henry, H. Lipson and W.A. Wooster, The Interpretation of X-ray Diffraction Photographs, MacMillan and Co., (1951).

29. A.D. Westland, private communication.

30. A. Anderson and P.R. Redfield, Phys. Rev., 116, 583 (1959).

31. M.H. Cohen and F. Reif, Solid State Physics, vol 5, ed. Seitz and Turnbull, Academic Press Inc., (1957).

32. G. Lamarche, to be published.

33. T. Jach, Appl. Phys. Letters, 28, 49 (1976)

34. B. Hébral, private communication.

APPENDIX

The Niomax wire level indicator for liquid helium is similar to the kind used at the C.R.T.B.T. laboratories in Grenoble, France[34].

The principle of operation is quite simple: the length of a superconducting wire in contact with the liquid helium is superconducting and the remainder, above, is normal and its resistance is nearly temperature independent. Therefore to know the level, one simply measures the resistance of the wire and determines the level since it is inversely proportional to the resistance.

To obtain such a behaviour, there are two important considerations. First, a superconducting wire having the right thermal conduction property must be chosen, and second, the measuring current must be optimized. To solve the first problem, Niomax wire consisting of a composite of multifilaments of a superconducting alloy in a copper-nickel matrix was suggested to us. Copper-nickel is known to be a relatively poor thermal conductor. The same composite in a copper matrix would probably not work for this purpose. The second requirement is easily found by experimentation when it is realized that for a particular level of helium in contact with the wire, there is a wide range of values of measuring currents for which the resistance is constant. This plateau in the R-I characteristic curve of the device gives the condition for the

optimum operating current. In our device, this was found to be around 120 mA. If the level indicator is operated much below 100 mA (eg. 40 mA), then the device loses its sensitivity to changes in level.

The circuit (See Fig.26) is a modified version of the C.R.T.B.T. circuit and was designed and built by A. Buser of our electronics shop. The circuit consists of a 24 V regulated power supply and a 100 mA constant current source. The voltage across the Niomax wire is measured with a galvanometer whose scale has been modified to read in centimeters of liquid level. It is equally possible to connect a digital voltmeter across the superconducting sensor for a more precise reading. With the galvanometer, it is possible to read the level to $\pm \frac{1}{2}$ cm while the digital voltmeter permits an accuracy of $\pm$ 1 mm. As it is found that during the initial transfer of the liquid helium, the surge of cold gas may cool the entire wire below its superconducting transition temperature, inspite of the measuring current flowing through. Some means of bringing the unimmersed part normal must be included in the circuit. For that purpose a large value capacitor was included in the electronics that can be switched on to supply a large current pulse down the wire to warm it and to resume normal operation of the level indicator.

The Niomax level indicator gives a consistently

accurate reading of the level, as has been confirmed by experimentation in glass dewars. It is thus more reliable and more precise than the carbon resistor variety of level detectors.

During an experiment, the level indicator may be operated continuously. It was found that the noise generated by it was quite negligible since it did not have any apparent effects on the operation of the SQUID which is very sensitive to its immediate environment. The loss of liquid helium on the other hand from the boiling caused by Joule heating (< 1 watt) is small and is removed by the escaping gas.

The wire is supported by a plastic rod that is slightly longer than the wire and is secured to the rod by passing it through several spacers made from pieces of Teflon tubing taped to the rod. The rod can then be mounted in any convenient place in the cryostat.

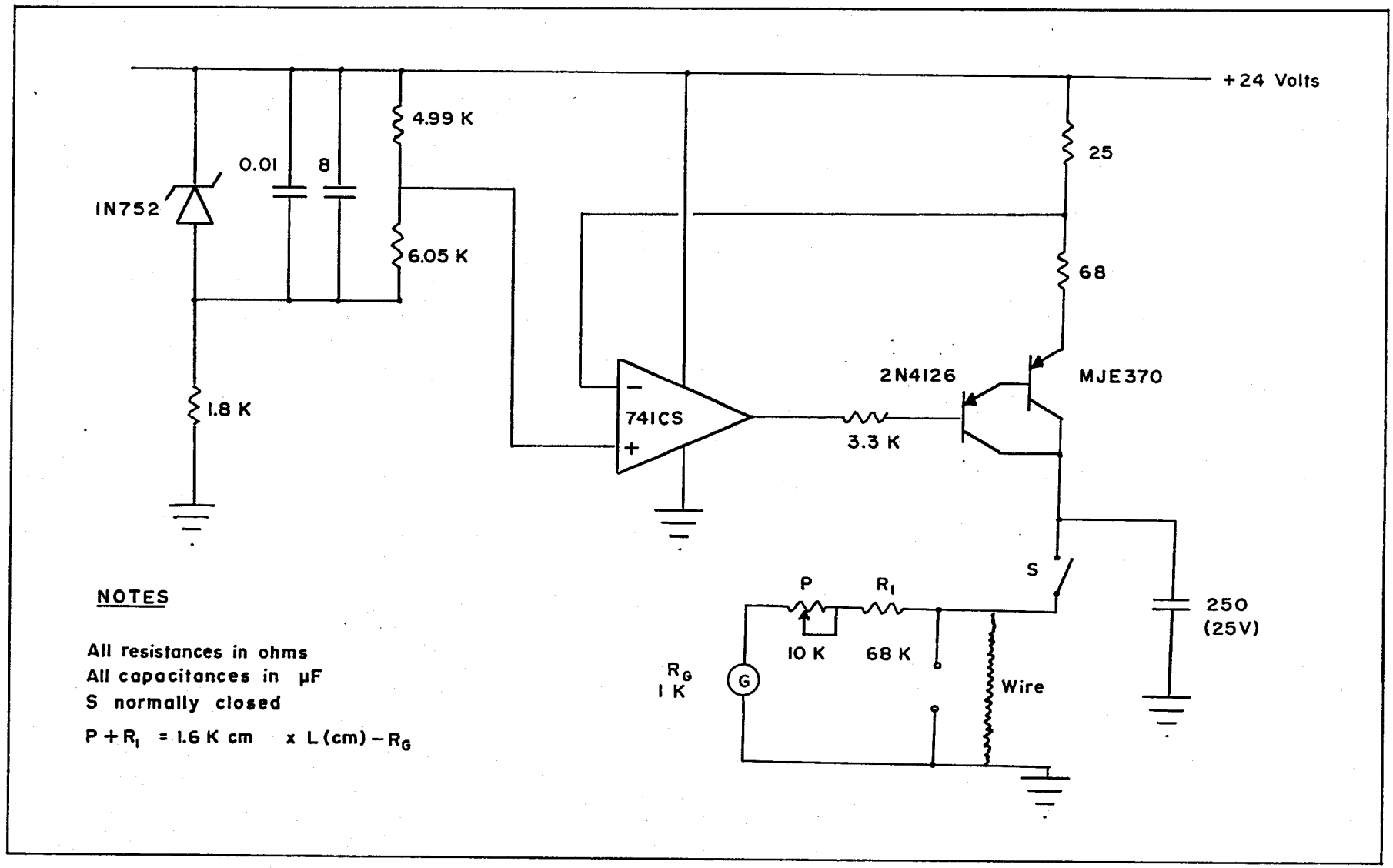

Fig. #26 Schematic of Liquid Helium Level Indicator

CALIBRATION TABLE OF C.R.T. UPPER

R	T	T_c*
960.4Ω	4.24K	4.24K
961.5	4.23	4.22
962.4	4.20	4.20
936.6	4.15	4.18
964.5	4.14	4.16
965.3	4.12	4.14
971.4	4.08	4.03
982.1	3.83	3.85
989.4	3.71	3.73
993.3	3.68	3.67
1000.3	3.56	3.56
1027.7	3.23	3.21
1083.0	2.68	2.67
1095.0	2.59	2.58
1107.0	2.49	2.49
1158.0	2.18	2.17
1180.0	2.05	2.06
1190.0	2.01	2.01
1210.0	1.915	1.920
1220.0	1.870	1.878
1230.0	1.832	1.837
1240.0	1.790	1.799
1250.0	1.745	1.762
1260.0	1.710	1.726

CALIBRATION TABLE OF C.R.T. UPPER

R	T	T_c*
1270.0Ω	1.673K	1.691K
1280.0	1.640	1.658
1290.0	1.572	1.626
1320.0	1.526	1.538
1338.8	1.483	1.487
1367.0	1.400	1.416
1377.0	1.379	1.392
1387.0	1.365	1.369
1396.2	1.349	1.349

* T_c calculated using

$$\frac{1}{T_c} = A - BR - CR^{\frac{1}{2}}$$

where A = -0.344263

B = 0.0016206

C = -0.0315042

CALIBRATION TABLE OF C.R.T. LOWER

From 4.242K to 1.397K

R	T	T_c*
825.4 Ω	4.242K	4.274K
827	4.223	4.226
835	4.009	4.000
840	3.892	3.871
845	3.777	3.749
850	3.669	3.635
855	3.563	3.527
860	3.455	3.426
865	3.373	3.330
870	3.281	3.239
875	3.197	3.153
880	3.104	3.072
885	3.036	2.994
890	2.960	2.920
895	2.888	2.850
900	2.818	2.783
910	2.703	2.658
920	2.583	2.543
930	2.474	2.437
940	2.375	2.340
950	2.285	2.250
960	2.193	2.167
970	2.110	2.089

CALIBRATION TABLE OF C.R.T. LOWER

From 4.242K to 1.397K

R	T	T_c*
980Ω	2.035K	2.017K
990	1.964	1.949
1000	1.898	1.886
1010	1.835	1.828
1020	1.777	1.771
1030	1.723	1.718
1040	1.671	1.669
1050	1.621	1.622
1060	1.577	1.577
1070	1.534	1.535
1080	1.493	1.495
1090	1.455	1.457
1100	1.417	1.421
1102	1.410	1.414
1106	1.397	1.400

* T_c is calculated using

$$\frac{1}{T_c} = A - BR - CR^{\frac{1}{2}}$$

where A = -0.6402545

B = 0.0022755

C = -0.0349439

From 239 mK to 1.12K

3336Ω	239 mK	239 mK
3325	240	240

CALIBRATION TABLE OF C.R.T. LOWER

From 239 mK to 1.12K

R	T	T_c*
3200Ω	250 mK	250 mK
3089	260	260
3042	265	265
2949	268	274
2977	269	271
2932	272	276
2925	276	277
2893	277	281
2916	279	278
2846	280	286
2816	286	290
2473	334	340
2360	352	362
2299	372	375
2029	447	448
1865	518	511
1820	526	532
1776	555	555
1762	570	563
1682	605	611
1647	665	636
1543	720	723
1509	765	758

CALIBRATION TABLE OF C.R.T. LOWER

From 239 mK to 1.12K

R	T	T_Ω*
1395Ω	905 mK	907 mK
1376	945	938
1318	1.05K	1.05K
1287	1.12	1.12

* T_c is calculated using

$$\frac{1}{T_c} = A - BR - CR^{\frac{1}{2}}$$

where A = -3.80945

B = 0.0003399

C = 0.118824